

Resonance chains and geometric limits on Schottky surfaces

Tobias Weich

March 30, 2022

Resonance chains have been observed in many different physical and mathematical scattering problems. Recently numerical studies linked the phenomenon of resonances chains to an approximate clustering of the length spectrum on integer multiples of a base length. A canonical example of such a scattering system is provided by 3-funneled hyperbolic surfaces where the lengths of the three geodesics around the funnels have rational ratios. In this article we present a mathematical rigorous study of the resonance chains for these systems. We prove the analyticity of the generalized zeta function which provide the central mathematical tool for understanding the resonance chains. Furthermore we prove for a fixed ratio between the funnel lengths and in the limit of large lengths that after a suitable rescaling, the resonances in a bounded domain align equidistantly along certain lines. The position of these lines is given by the zeros of an explicit polynomial which only depends on the ratio of the funnel lengths.

Contents

1	Introduction	2
2	Resonances and zeta functions for Schottky surfaces	5
3	Dynamical zeta functions for iterated function schemes	7
4	Flow-adapted iterated function schemes and generalized zeta functions	12
5	Geometric limits	23
6	Numerical Illustration	38

1 Introduction

Let $X = \Gamma \backslash \mathbb{H}$ be a convex co-compact hyperbolic surface, then this surface has infinite volume, finite genus and a finite number of funnels. The resolvent of the positive Laplacian Δ_X is usually defined as

$$R(s) = (\Delta_X - s(s-1))^{-1},$$

and on $L^2(X)$ it is analytic in s for $\operatorname{Re}(s) > 1$. Changing the function spaces this resolvent can be meromorphically extended to $s \in \mathbb{C}$ with poles of finite rank. The poles of this meromorphic continuation are called the resonances of X and the multiplicity of a resonance is defined by the rank of the associated pole. The set of all resonances on X repeated according to multiplicity will be called $\operatorname{Res}(X)$.

The study of the distribution of resonances on infinite volume hyperbolic surfaces is of interest in number theory (see e.g. the recent work of Bourgain-Gamburd-Sarnak [7] on the affine sieve) as well as in the study of quantum chaos, because these surfaces provide an important model of open, classically chaotic systems (see [21] for a recent review).

Since the seminal work of Patterson it is known that there is always one resonance at $s = \delta$, where δ is the Hausdorff dimension of the limit set $\Lambda(\Gamma)$ (see [22] for $\delta > 1/2$ and [23] for $\delta \leq 1/2$). For the hyperbolic cylinder even the complete resonance spectrum can be computed, but apart from this special example there are no other explicit formulas for the location of individual resonances.

However, it has been a very fruitful approach to prove coarser results on the distribution of resonances in the complex plane. For example Guillopé-Lin-Zworski [13] proved a fractal Weyl upper bound on the number of resonances near the critical line

$$\#\{s \in \operatorname{Res}(X), r \leq |\operatorname{Im}(s)| \leq r+1 \text{ and } \operatorname{Re}(s) > -C\} = O(r^\delta)$$

and Naud [20] the existence of a spectral gap, i.e. of a constant $\varepsilon > 0$ such that

$$\{s \in \operatorname{Res}(X), \operatorname{Re}(s) > \delta - \varepsilon\} = \{\delta\}.$$

Such asymptotic results on the resonance distribution have important analogons in theoretical physics [10, 17, 27] and are even observable experimentally [2, 25]. Despite the big progress in recent years there are still many open questions and conjectures. For example it has been conjectured that the fractal Weyl upper bound is sharp and that, in the semiclassical limit, i.e. for $\operatorname{Im}(s) \rightarrow \infty$ the spectral gap can be extended to $\delta/2$. For a more thorough discussion on recent progress on the distribution of resonances and open questions we refer to [21] and references therein.

The existence of these open conjectures motivated Borthwick to study the resonance spectrum on infinite volume hyperbolic surfaces numerically [4] and to a great surprise he observed that the resonances on 3-funneled Schottky surfaces are often highly ordered and form resonance chains. It has recently been shown in a numerical study by Barkhofen, Faure and the author [1] that these resonance chains can be understood by a generalized zeta function and are related to a clustering of the length spectrum

on X and that the same kind of resonance chains also appear in various other physical systems (for details on the significance of resonance chains in physics we refer to [30] and references therein).

Statement of the results: In this article we will show the existence of resonance chains for 3-funneled surfaces by proving explicit formulas for individual resonances in a certain geometrical limit in the Teichmüller space. A 3-funneled Schottky surface of genus zero is up to isometry uniquely defined by three positive real numbers l_1, l_2, l_3 which correspond to the funnel widths i.e. the lengths of the primitive closed geodesics that turns once around one funnel. The numbers l_1, l_2, l_3 are also called Fenchel-Nielsen coordinates of the Teichmüller space of 3-funneled surfaces (cf. [3, Section 13.3]) and we will denote these surfaces by X_{l_1, l_2, l_3} . Let $n_1, n_2, n_3 \in \mathbb{N}$ be positive integers, then we consider for $\ell > 0$ the family of Schottky surfaces

$$X_{n_1, n_2, n_3}(\ell) := X_{n_1 \ell, n_2 \ell, n_3 \ell}$$

with a fixed rational ratio of the funnel widths. In the limit $\ell \rightarrow \infty$ the system becomes more and more open and the dimension of the limit set tends to zero $\delta \rightarrow 0$. One observes that in this limit not only the leading resonance at δ tends to zero but all other resonances do as well. In order to study a meaningful, nontrivial limit of the resonance spectrum, the spectrum has to be rescaled with ℓ and we define the set of rescaled resonances as

$$\widetilde{\text{Res}}_{n_1, n_2, n_3}(\ell) := \{s \in \mathbb{C}, s/\ell \in \text{Res}(X_{n_1, n_2, n_3}(\ell))\}.$$

Then we obtain the following theorem for the rescaled resonances in the limit $\ell \rightarrow \infty$.

Theorem 1.1. *Let n_1, n_2, n_3 be positive integers that fulfill a triangle condition i.e. they fulfill the inequality $n_i + n_j > n_k$ for any permutation of 1, 2, 3. Let furthermore be*

$$P_{n_1, n_2, n_3}(x) := 1 - 2(x^{n_1} + x^{n_2} + x^{n_3}) + x^{2n_1} + x^{2n_2} + x^{2n_3} + 2(x^{n_1+n_2} + x^{n_2+n_3} + x^{n_1+n_3}) - 4x^{n_1+n_2+n_3} \quad (1.1)$$

and

$$\mathcal{N}_{n_1, n_2, n_3} := \{s \in \mathbb{C}, P_{n_1, n_2, n_3}(e^{-s}) = 0\}$$

where the zeros are repeated according to the multiplicities. Then for any bounded domain $U \subset \mathbb{C}$ with $\partial U \cap \mathcal{N}_{n_1, n_2, n_3} = \emptyset$ we have

$$\lim_{\ell \rightarrow \infty} \#(U \cap \widetilde{\text{Res}}_{n_1, n_2, n_3}(\ell)) = \#(U \cap \mathcal{N}_{n_1, n_2, n_3}).$$

Note that U can be chosen arbitrarily small, so Theorem 1.1 states that a finite number of resonances is determined by P_{n_1, n_2, n_3} at an arbitrary precision for large enough ℓ . As $\mathcal{N}_{n_1, n_2, n_3}$ is the zero set of a polynomial in e^{-s} , this set naturally forms straight chains in the sense that

$$s_0 \in \mathcal{N}_{n_1, n_2, n_3} \Rightarrow s_k = s_0 + 2\pi i k \in \mathcal{N}_{n_1, n_2, n_3}, \quad \forall k \in \mathbb{Z}.$$

Theorem 1.1 then says that the rescaled resonance spectrum converges against straight resonance chains which are explicitly described by the polynomial P_{n_1, n_2, n_3} . Note that this convergence however only holds for an arbitrarily large but finite number of resonances and one can not suspect Theorem 1.1 to hold uniformly for all resonances because this would contradict the fractal Weyl conjecture on the number of resonances in the semiclassical limit. The limit $\ell \rightarrow \infty$ thus can be understood as a limit complementary to the semiclassical limit which holds in the low frequency regime i.e. for a finite number of resonances. And in fact we will see in Section 6 that P_{n_1, n_2, n_3} describes the first 50-100 resonances already for relatively small values of $\ell \approx 4$.

In the proof of Theorem 1.1 a generalized dynamical zeta function will play an important role and we will show that such generalized zeta functions always have an analytic extension. Therefore we introduce $\mathcal{P}_{X_{l_1, l_2, l_3}}$ as the set of all primitive closed geodesics on X_{l_1, l_2, l_3} , where primitive means that the geodesic is not a repetition of a shorter closed geodesic. If we additionally denote for a closed geodesic γ its length by $l(\gamma)$ then we can state the following result.

Theorem 1.2. *Let X_{l_1, l_2, l_3} be a Schottky surface with three funnels of widths l_1, l_2, l_3 and let $n_1, n_2, n_3 \in \mathbb{N}$. We define*

$$\mathbf{n} : \begin{cases} \mathcal{P}_{X_{l_1, l_2, l_3}} & \rightarrow \mathbb{N} \\ \gamma & \mapsto \sum_{i=1}^3 n_i w_i(\gamma) \end{cases} \quad (1.2)$$

where $w_i(\gamma)$ denotes the winding number around the funnel of width l_i . Then the generalized zeta function

$$d_{\mathbf{n}}(s, z) = \prod_{\gamma \in \mathcal{P}_{X_{l_1, l_2, l_3}}} \prod_{k \geq 0} \left(1 - z^{\mathbf{n}(\gamma)} e^{-(k+s)l(\gamma)} \right). \quad (1.3)$$

extends to an analytic function on \mathbb{C}^2 .

Similar to an ordinary dynamical zeta function, obtained by a Bowen-Series transfer operator, this generalized zeta function is equal to the Selberg zeta function of X_{l_1, l_2, l_3} for $z = 1$. Beside its appearance in the proof of Theorem 1.1 this result is also of independent interest as in [1] it has been numerically shown that for the understanding of the resonance chains for finite ℓ these generalized zeta functions are the central object. The numerical algorithms used in [1] and the interpretation of the results were also heavily based on the assumption that the generalized zeta function is analytic.

The particularly simple structure of the resonance spectrum in the limit $\ell \rightarrow \infty$ as stated in Theorem 1.1 can finally be understood by the following result which states that in the limit $\ell \rightarrow \infty$ the generalized zeta function of Theorem 1.2 is given by the polynomial P_{n_1, n_2, n_3} .

Theorem 1.3. *Let n_1, n_2, n_3 be positive integers fulfilling the triangle condition. Consider for $\ell > 0$ the family of Schottky surfaces $X_{n_1, n_2, n_3}(\ell)$ then the generalized zeta function of this family of surfaces, as defined in Theorem 1.2, also depends on the parameter ℓ and we denote it by $d_{\mathbf{n}}(s, z; \ell)$. If P_{n_1, n_2, n_3} is the polynomial defined in (1.1),*

then on any bounded set $B \subset \mathbb{C}^2$ the rescaled generalized zeta function $d_{\mathbf{n}}(z, s/\ell; \ell)$ converges to the polynomial in the sense that

$$\lim_{\ell \rightarrow \infty} \|d_{\mathbf{n}}(z, s/\ell; \ell) - P_{n_1, n_2, n_3}(ze^{-s})\|_{\infty, B}. \quad (1.4)$$

The article is organized as follows: First we will recall some basic facts on the definition of Schottky surfaces, their resonances and Selberg zeta functions in Section 2. Then, in Section 3, we recall the definition of the dynamical zeta function the way they are usually obtained using Bowen-Series maps and iterated function schemes (IFS). While this traditional approach is very natural from an algebraic point of view, we will see that it is not natural from the geodesic flow point of view. Section 4 will then be dedicated to an iterated function scheme whose dynamical zeta function also contain the Selberg zeta function of the Schottky surface but that is much better adapted to the geodesic flow. These *flow-adapted IFS* are then used to prove Theorem 1.2 on the analyticity of the generalized zeta functions. The flow-adapted IFS in addition turn out to be the central ingredient in treating the limit $\ell \rightarrow \infty$ in Section 5. The idea in proving Theorem 1.1 and Theorem 1.3 is to write the generalized zeta function as a Fredholm determinant of a transfer operator defined by the flow-adapted IFS. If one then considers the Taylor expansion of this Fredholm determinant it can be shown using techniques from Jenkinson-Pollicott [15], that in the limit $\ell \rightarrow \infty$ only the first view terms survive. Furthermore all remaining terms become particularly simple and cancel each other to a great extend. From a physical point of view the proof strategy is to show that the ideas which Cvitanovic-Eckhardt [9] introduced under the name “cycle expansion” in physics become rigorous in the limit $\ell \rightarrow \infty$ on Schottky surfaces. Finally, in Section 6 we will compare the results with numerical calculations and we will observe that the resonances in the low-frequency regime are already surprisingly well described by P_{n_1, n_2, n_3} for relatively small values of ℓ ($\ell \approx 4$) which illustrates the practical value of Theorem 1.1.

Acknowledgements: I am grateful to Frédéric Faure who proposed to study these geometric limits and motivated me to start this work. The discussions with him were a constant source of inspiration throughout this work. I am also thankful to David Borthwick and Pablo Ramacher for helpful discussions and corrections of an early stage of this article. This work was supported by the German National Academic Foundation and by the Agence National de Recherche via the project 2009-12 METHCHAOS.

2 Resonances and zeta functions for Schottky surfaces

All hyperbolic surfaces can be written as a quotient of the hyperbolic half plane \mathbb{H} by a discrete subgroup of its orientation preserving isometry group $\Gamma \subset \text{Isom}^+(\mathbb{H}) = \text{PSL}(2, \mathbb{R})$. We will be particularly interested in Schottky surfaces which are quotients by certain freely generated groups, called Schottky groups. These groups can be defined as follows.

Definition 2.1. Let D_1, \dots, D_{2r} be disjoint open disks in \mathbb{C} with centers on the real line and mutually disjoint closures. Then there exists for each pair D_i, D_{i+r} a

hyperbolic element $S_i \in PSL(2, \mathbb{R})$ that maps ∂D_i to ∂D_{i+r} and that maps the interior of D_i to the exterior of D_{i+r} . A *Schottky group* is then the free group generated by S_1, \dots, S_r .

With this definition Schottky surfaces are always surfaces of infinite volume without cusps and with a finite number of funnels. The simplest nontrivial example of Schottky surfaces are those surfaces with three funnels of genus zero (see upper part of Figure 4.1). Given three positive real numbers l_1, l_2, l_3 a Schottky group of such a surface is freely generated by the two hyperbolic elements

$$S_1 = \begin{pmatrix} \cosh(l_1/2) & \sinh(l_1/2) \\ \sinh(l_1/2) & \cosh(l_1/2) \end{pmatrix}, \quad S_2 = \begin{pmatrix} \cosh(l_2/2) & a \sinh(l_2/2) \\ a^{-1} \sinh(l_2/2) & \cosh(l_2/2) \end{pmatrix}, \quad (2.1)$$

where the parameter a is chosen such that $\text{Tr}(S_1 S_2^{-1}) = -2 \cosh(l_3/2)$. We write

$$\Gamma_{l_1, l_2, l_3} := \langle S_1, S_2 \rangle \text{ and } X_{l_1, l_2, l_3} := \Gamma_{l_1, l_2, l_3} \backslash \mathbb{H}.$$

The parameters l_1, l_2, l_3 coincide with the lengths of the three primitive closed geodesics around the three funnels of the surface X_{l_1, l_2, l_3} (see the geodesics γ_1, γ_2 and γ_3 in Figure 4.1) and parametrize uniquely all hyperbolic surfaces of this type. They are also called Fenchel-Nielsen coordinates because they are global coordinates on the Teichmüller space for 3-funneled surfaces of genus zero, i.e. the space of all isometry classes of hyperbolic metrics on this surface (cf. [3, Section 13.3]).

The spectral properties of a general Schottky surface X are described by the positive Laplacian Δ_X . As the surface has infinite volume it is known that it has at most finitely many L^2 -eigenvalues in $(0, 1/4)$ and absolutely continuous spectrum on $[1/4, \infty)$ with no embedded eigenvalues. The L^2 -spectrum thus is not a good spectral quantity and it is well known that instead one has to study the resonances of the Laplace operator. These resonances can be defined by the meromorphic continuation of the resolvent which has been shown by Mazzeo-Melrose [18] and Guilloupe-Zworski [14]

Theorem 2.2. *The resolvent*

$$R_X(s) := (\Delta_X - s(1-s))^{-1} : L^2(X) \rightarrow H^2(X)$$

which is defined for $\text{Re}(s) \geq 1/2$ and $s(1-s) \notin \text{spec}(\Delta_X)$ extends to a meromorphic family of operators

$$R_X(s) : L^2_{\text{comp}}(X) \rightarrow H^2_{\text{loc}}(X)$$

with poles of finite rank.

By this meromorphic continuation we can define the set of resonances as

$$\text{Res}(X) := \{s \in \mathbb{C}, s \text{ is pole of } R_X(s), \text{ repeated according to multiplicity}\}. \quad (2.2)$$

Surfaces with constant negative curvature have the remarkable property that their resonance spectrum is related to the zeros of their Selberg zeta function which we introduce now. If γ is a closed geodesic on a hyperbolic surface X we can

create longer closed geodesics by simply repeating it. We call a geodesic *primitive* if it cannot be obtained as a repetition of a shorter geodesic and we denote the *set of primitive closed geodesics* on X by

$$\mathcal{P}_X := \{\gamma, \text{ closed primitive geodesic on } X\}.$$

If $l(\gamma)$ denotes the length of a geodesic γ , then the *Selberg zeta function* of X is defined as

$$Z_X(s) := \prod_{\gamma \in \mathcal{P}_X} \prod_{k \geq 0} \left(1 - e^{-(s+k)l(\gamma)}\right). \quad (2.3)$$

This product is absolutely convergent for $\operatorname{Re}(s)$ sufficiently large and for Schottky surfaces it extends to an analytic function on \mathbb{C} [12]. The result of Patterson-Perry [24] which was later generalized to surfaces with cusps by Borthwick-Judge-Perry [5] (see also Bunke-Olbrich [8]) relates the resonances to the zeros of the Selberg zeta function.

Theorem 2.3. *For a Schottky surface $X = \Gamma \backslash \mathbb{H}$ the zero set of the zeta function $Z_X(s)$ is the union of the resonances $\operatorname{Res}(X)$ and the negative integers $s = -k$, $k \in \mathbb{N}_0$.*

3 Dynamical zeta functions for iterated function schemes

The correspondence between the zeros of the Selberg zeta function and the resonances as stated in Theorem 2.3 is a central ingredient for understanding the resonance chains. However we first have to develop a different point of view on the Selberg zeta function by the so called dynamical zeta function, which we introduce in this section for holomorphic iterated function schemes.

Definition 3.1 (Holomorphic iterated function scheme). For $N \in \mathbb{N}$ let $D_1, \dots, D_N \subset \mathbb{C}$ be N open disks such that their closures \overline{D}_i are pairwise disjoint. Let $A \in \{0, 1\}^{N \times N}$ be the *adjacency matrix* and denote $i \rightsquigarrow j$ if $A_{i,j} = 1$. Furthermore for each pair $(i, j) \in \{1, \dots, N\}^2$ with $i \rightsquigarrow j$ we have a biholomorphic map $\phi_{i,j} : D_i \mapsto \phi_{i,j}(D_i)$ such that $\phi_{i,j}(D_i) \Subset D_j$ and such that different images are pairwise disjoint, i.e.

$$\phi_{i,j}(D_i) \cap \phi_{k,l}(D_k) \neq \emptyset \Leftrightarrow i = k \text{ and } j = l. \quad (3.1)$$

Finally we call a holomorphic IFS *eventually contracting*, if there is a N_0 and $\theta < 1$ such that for $n \geq N_0$

$$|\phi'_w(u)| \leq \theta \text{ for all } w \in \mathcal{W}_n \text{ and } u \in D_{w_0}.$$

For convenience we denote the union of all the disjoint disks by

$$D := \bigcup_i D_i$$

and the union of all their images by

$$\phi(D) := \bigcup_{i \rightsquigarrow j} \phi_{i,j}(D_i).$$

From (3.1) it follows directly that for $u \in \phi(D)$ there is exactly one pair $i \rightsquigarrow j$ and $u' \in D_i$ such that $u = \phi_{i,j}(u')$. We have thus a well defined holomorphic inverse function

$$\phi^{-1} : \phi(D) \rightarrow D.$$

Example 3.2. The disks D_i and generators S_i in the construction of a Schottky group (see Definition 2.1) give a natural construction of a holomorphic IFS. For convenience we denote for $i = 1, \dots, r$ $S_{i+r} := S_i^{-1}$ and use a cyclic notation of the indices i.e. $S_{i+2r} = S_i$ and $D_{i+2r} = D_i$. Then for $i = 1, \dots, r$ all elements S_i map all disks, except D_i , holomorphically into the interior of D_{i+r} . Thus the adjacency matrix of this IFS is given by a $2r \times 2r$ matrix with $A_{i,j} = 0$ if $|i - j| = r$ and $A_{i,j} = 1$ else. For any $i \rightsquigarrow j$ the maps are given by

$$\phi_{i,j}(u) := S_{j+r}u = S_j^{-1}u.$$

They clearly fulfill (3.1) and are also known to be eventually contracting (see e.g. [3, Proposition 15.4]). Note that the inverse map ϕ^{-1} restricted to $D_j \cap \phi(D)$ is exactly given by S_j . The IFS which we defined is consequently the inverse of the usual *Bowen-Series map* for Schottky groups (see e.g. [3, Section 15.2]).

It will turn out to be useful for the notation to introduce the following symbolic coding. The *symbols* are given by the integers $1, \dots, N$ and the set of words of length n by the tuples of symbols

$$\mathcal{W}_n := \{(w_0, \dots, w_n), w_i \rightsquigarrow w_{i+1} \text{ for all } i = 0, \dots, n-1\}.$$

Note that our notation of *word length* does not refer to the number of symbols, but to the number of transitions $w_i \rightsquigarrow w_{i+1}$ which they indicate. For $w \in \mathcal{W}_n$ and $0 < k \leq n$ we define the *truncated word* by

$$w_{0,k} := (w_0, \dots, w_k) \in \mathcal{W}_k.$$

Finally we define the iteration of the maps $\phi_{i,j}$ along a word $w \in \mathcal{W}_n$ as

$$\phi_w := \phi_{w_{n-1}, w_n} \circ \dots \circ \phi_{w_0, w_1} : D_{w_0} \mapsto D_{w_n}$$

and their images as

$$D_w := \phi_w(D_{w_0}).$$

Note that $D_w \Subset D_{w_n}$ and that from the separation condition (3.1) one obtains inductively for $w, w' \in \mathcal{W}_n$

$$D_w \cap D_{w'} \neq \emptyset \Leftrightarrow w = w'.$$

We call a word $w \in \mathcal{W}_n$ of length n *closed* if $w_0 = w_n$ and we denote the set of all closed words of length n by \mathcal{W}_n^{cl} . Given a closed word $w \in \mathcal{W}_n^{cl}$, the map

$$\phi_w : D_{w_0} \rightarrow D_w \subseteq D_{w_0}$$

of an eventually contracting IFS has a unique fixed point (see e.g. [6, Lemma 2.3]) which we denote by u_w . If a closed word $w \in \mathcal{W}_n^{cl}$ of length n is concatenated k -times with itself, we obtain a closed word of length $k \cdot n$

$$w^k = (w_0, w_1, \dots, w_{n-1}, w_0, \dots, \dots, w_{n-1}, w_0, \dots, w_{n-1}, w_0) \in \mathcal{W}_{nk}^{cl}.$$

In analogy to the primitive closed geodesics, we call a word w *prime* if it can not be obtained by the repetition of a shorter word and we write

$$\mathcal{W}_n^{\text{prime}} := \{w \in \mathcal{W}_n^{cl}, w \text{ is prime}\}.$$

Note that as well the set of closed words as the set of prime words is invariant under the left-shift

$$\sigma_L : \begin{cases} \mathcal{W}_n^{cl/\text{prime}} & \rightarrow \mathcal{W}_n^{cl/\text{prime}} \\ (w_0, \dots, w_{n-1}, w_0) & \mapsto (w_1, \dots, w_{n-1}, w_0, w_1) \end{cases}.$$

and the right-shift

$$\sigma_R : \begin{cases} \mathcal{W}_n^{cl/\text{prime}} & \rightarrow \mathcal{W}_n^{cl/\text{prime}} \\ (w_0, \dots, w_{n-1}, w_0) & \mapsto (w_{n-1}, w_0, \dots, w_{n-1}, w_{n-1}) \end{cases}.$$

obviously $\sigma_L^{-1} = \sigma_R$ and iterative application of these operators induce a \mathbb{Z} -action on the set of words. The importance of this shift action arises from the fact that on the periodic orbits, the dynamics of the IFS is conjugated to the dynamics of the shift operator on the closed words in the following sense

$$\forall w \in \mathcal{W}_n^{cl}, 0 < k < n : \phi_{w_0, k}(u_w) = u_{\sigma_L^k w}. \quad (3.2)$$

We will denote by $[w]$ the orbit of a word w by this \mathbb{Z} -action on $\mathcal{W}_n^{cl/\text{prime}}$ and write the space of these orbits, i.e. the quotient by the group action as

$$\left[\mathcal{W}_n^{cl/\text{prime}} \right] := \mathbb{Z} \backslash \mathcal{W}_n^{cl/\text{prime}}.$$

Next we define the transfer operators associated to the iterated function schemes.

Definition 3.3. Let $\mathcal{A}_\infty(D)$ be the Banach space of holomorphic functions on D that are bounded on \overline{D} with the supremum norm. If we have a function $V \in \mathcal{A}_\infty(\phi(D))$ then we define the *transfer operator* $\mathcal{L}_V : \mathcal{A}_\infty(D) \rightarrow \mathcal{A}_\infty(D)$ associated to the IFS by

$$(\mathcal{L}_V h)(u) := \sum_{i=1}^N (\mathcal{L}_V^{(i)} h)(u) \quad (3.3)$$

where

$$\mathcal{L}_V^{(i)} : \begin{cases} \mathcal{A}_\infty(D) & \rightarrow \mathcal{A}_\infty(D_i) \\ h(u) & \mapsto (\mathcal{L}_V^{(i)}h)(u) := \sum_{j \text{ s.t. } i \rightsquigarrow j} V(\phi_{i,j}(u))h(\phi_{i,j}(u)) \end{cases} \quad (3.4)$$

The sum in (3.3) is then understood in the sense that $\mathcal{A}_\infty(D) = \bigoplus_{i=1}^N \mathcal{A}_\infty(D_i)$.

Given such a potential V , a word $w \in \mathcal{W}_n$ and a point $u \in D_{w_0}$, we can define the iterated product

$$V_w(u) := \prod_{k=1}^n V(\phi_{w_0,k}(u)). \quad (3.5)$$

A straight forward calculation of powers of the transfer operator \mathcal{L}_V leads to

$$(\mathcal{L}_V^n h)(u) = \sum_{w \in \mathcal{W}_n, \text{ s.t. } u \in D_{w_0}} V_w(u)h(\phi_w(u)),$$

thus these iterated products naturally occur in powers of \mathcal{L}_V .

Definition 3.4. An operator $\mathcal{L} : \mathcal{B} \rightarrow \mathcal{B}$ on a Banach space \mathcal{B} is called *nuclear*, if there exist $v_n \in \mathcal{B}$, $\alpha_n \in \mathcal{B}^*$ with $\|v_n\| = \|\alpha_n\| = 1$ and $\lambda_n \in \mathbb{C}$ with $\sum_{n=0}^{\infty} |\lambda_n| < \infty$ such that

$$\mathcal{L}h = \sum_{n=0}^{\infty} \lambda_n \alpha_n(h) v_n \quad (3.6)$$

for any $h \in \mathcal{B}$. The representation (3.6) is then called *nuclear representation* of \mathcal{L} .

It is a well known fact that these transfer operators of holomorphic IFS are nuclear operators (see [26] or [15, Proposition 2], respectively) and that for eventually contracting IFS the trace can be expressed in terms of the points u_w . Accordingly one can define the *dynamical zeta function* by the Fredholm determinant

$$d_V(z) := \det(1 - z\mathcal{L}_V) \quad (3.7)$$

which is an entire function on \mathbb{C} and which can be written for $|z|$ sufficiently small as (see e.g. [15, (3.26)])

$$d_V(z) = \exp \left(- \sum_{n>0} \frac{z^n}{n} \sum_{w \in \mathcal{W}_n^{cl}} V_w(u_w) \frac{1}{1 - \phi'_w(u_w)} \right). \quad (3.8)$$

One has the following important connection between the dynamical and Selberg zeta function:

Theorem 3.5. *Let $X = \Gamma \backslash \mathbb{H}$ be a Schottky surface and take the iterated function scheme associated to the Bowen-Series maps as defined in Example 3.2. For $s \in$*

\mathbb{C} define the potential $V_s(z) = [(\phi^{-1})'(z)]^{-s}$ and consider the holomorphic family of nuclear operators \mathcal{L}_{V_s} . Then the dynamical zeta function

$$d(s, z) := \det(1 - z\mathcal{L}_{V_s})$$

is holomorphic in both variables and

$$Z_X(s) = d(s, 1).$$

Proof. We will only give a sketch of the proof here, considering those steps which will be of further importance in this article. For a detailed proof see e.g. [3, Theorem 15.8].

The proof heavily relies on a product form of the general dynamical zeta function which we will derive now. Expanding the last quotient in (3.8) as a geometric series one obtains

$$d_V(z) = \exp \left(- \sum_{k \geq 0} \sum_{n > 0} \sum_{w \in \mathcal{W}_n^{cl}} \frac{z^n}{n} V_w(u_w) (\phi'_w(u_w))^k \right).$$

Next one checks that for a given class of words $[w] \in [\mathcal{W}_n^{cl}]$ neither $V_w(u_w)$ nor $\phi'_w(u_w)$ depend on the choice of the representative w . Furthermore one easily calculates that

$$V_{w^k}(u_{w^k}) = (V_w(u_w))^k \text{ and } \phi'_{w^k}(u_{w^k}) = (\phi'_w(u_w))^k.$$

Consequently the sum over all closed words represented by the double sum $\sum_{n > 0} \sum_{w \in \mathcal{W}_n^{cl}}$ can be transformed into a sum over all classes of prime words and their repetitions and one obtains

$$d_V(z) = \exp \left(- \sum_{k \geq 0} \sum_{r > 0} \sum_{[w] \in [\mathcal{W}^{\text{prime}}]} \frac{\left(z^{n_w} V_w(u_w) (\phi'_w(u_w))^k \right)^r}{r} \right).$$

where $[\mathcal{W}^{\text{prime}}] = \bigcup_n [\mathcal{W}_n^{\text{prime}}]$ is the set of the prime word-classes of arbitrary length and n_w denotes the length of the word w . Finally using the Taylor expansion $\log(1 - x) = - \sum_{r > 0} x^r / r$ one obtains

$$d_V(z) = \prod_{[w] \in [\mathcal{W}^{\text{prime}}]} \prod_{k \geq 0} \left(1 - z^{n_w} V_w(u_w) (\phi'_w(u_w))^k \right). \quad (3.9)$$

With the special choice of the potential $V_s(u) = ((\phi^{-1})'(u))^{-s}$ one then obtains

$$d(s, z) = \prod_{[w] \in [\mathcal{W}^{\text{prime}}]} \prod_{k \geq 0} \left(1 - z^{n_w} (\phi'_w(u_w))^{s+k} \right).$$

The equivalence to the Selberg zeta function then follows from a one-to-one correspondence between the classes of prime words of the Bowen-Series IFS and the primitive geodesics on the Schottky surfaces (see e.g. [3, Proposition 15.5]) and from the fact that the stabilities of the fixed points $\phi'_w(u_w)$ are related to the lengths of these geodesics. \square

As explained in Section 2 we are especially interested in zeros of the zeta function. The fixed point formula (3.8) for the dynamical zeta function can however not vanish if the series are absolutely convergent. But the fixed point formula (3.8) is only valid in the region of absolute convergence, in the rest of the complex plane the zeta function is only defined by analytic continuation. Equation (3.8) is thus only valid in a region where the zeta function has no zeros. The same is true for the product formula (2.3) of the Selberg zeta functions. Both formulas are thus not at all useful for determining the zeros numerically. One can however use the following clever trick which has been introduced in physics by Cvitanovic-Eckhardt [9] under the name *cycle expansion* and that has been rigorously applied to Schottky surfaces by Jenkinson-Pollicott [15] in mathematics: As for any bounded potential V the series in (3.8) converges in a neighborhood of zero, one can derive a general formula for the Taylor coefficients of the Taylor expansion of $d_V(z)$ in z around zero. This expansion is given by [15, Proposition 8]:

$$d_V(z) = 1 + \sum_{N=1}^{\infty} z^N d_V^{(N)} \quad (3.10)$$

with

$$d_V^{(N)} = \sum_{m=1}^N \left(\sum_{(n_1, \dots, n_m) \in P(N, m)} \frac{(-1)^m}{m!} \prod_{l=1}^m \frac{1}{n_l} \sum_{w \in \mathcal{W}_{n_l}^{cl}} \frac{V_w(u_w)}{1 - \phi'_w(u_w)} \right) \quad (3.11)$$

where $P(N, m)$ is the set of all m -partitions of N , i.e. the set of all integer m -tuples that sum up to N . As $d_V(z)$ is known to be analytic on all \mathbb{C} its Taylor expansion (3.10) converges absolutely on \mathbb{C} and is well suited for numerical calculations of its zeros (c.f. [4]).

4 Flow-adapted iterated function schemes and generalized zeta functions

As mentioned in the proof of Theorem 3.5 the key ingredient for the equivalence between the dynamical zeta function of the standard Bowen-Series IFS and the Selberg zeta function is an equivalence between periodic geodesics on the surface and periodic orbits of the IFS. This equivalence is usually proven in a purely algebraic way by arguing with conjugacy classes in the Schottky group Γ . This equivalence can however also be understood from a geometric or dynamical point of view by interpreting the Bowen-Series maps as some kind of Poincaré section of the geodesic flow. The 3-funneled Schottky surface can be obtained from its fundamental domain by gluing together the circles of the same color (see Figure 4.1). Each closed geodesic on the surface crosses the blue and red cut lines a finite number of times and can be represented by one or several arcs in the fundamental domain. The fixed points of the Bowen-Series map are then exactly the end-points of these arcs. We do not want to go any further into details, as we will need no rigorous statement of this correspondence in

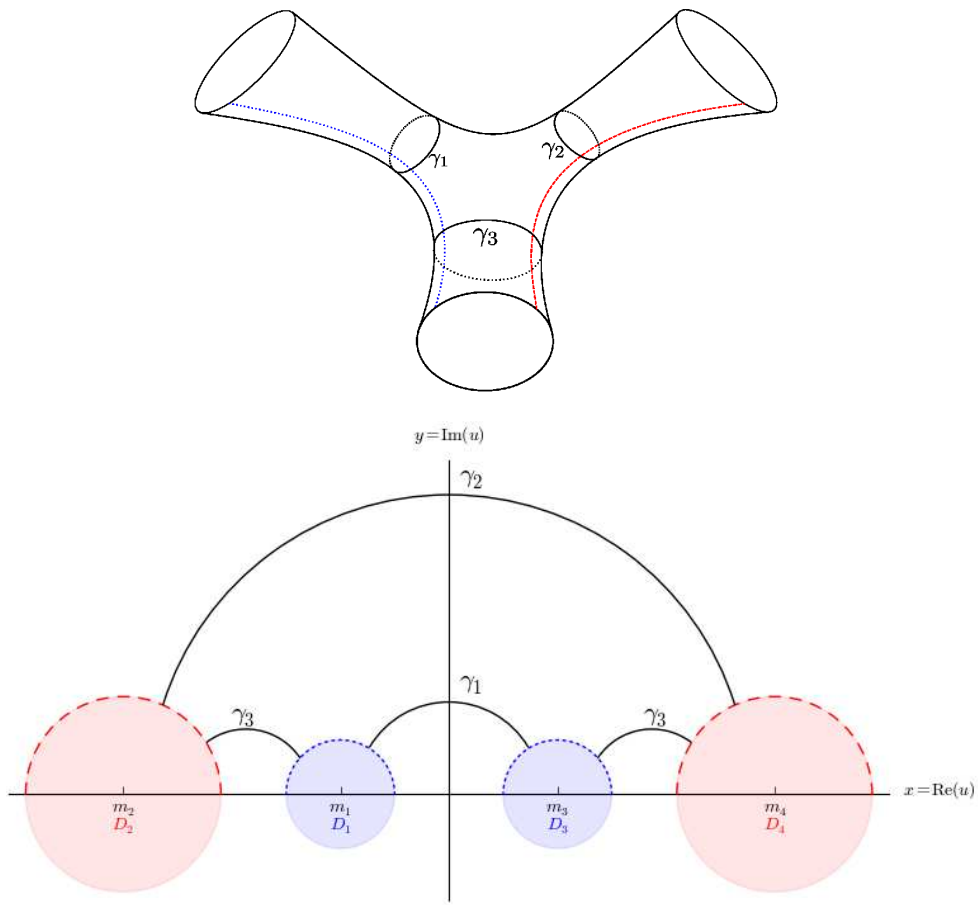


Figure 4.1: Upper part: Schematic sketch of a 3-funneled Schottky surface. The dashed red and dotted blue line indicate the cut lines which would correspond to the Poincaré section of the standard Bowen-Series IFS. The black lines represent the three fundamental geodesics that wind one time around one of the funnels. Lower part: Configuration of 4 disks that give rise to the construction of a 3-funneled Schottky surface. The upper half plane without the disks represents a fundamental domain and the surface can be obtained by gluing together the two red dashed lines and the two blue dotted lines. In black the three fundamental closed geodesics $\gamma_1, \gamma_2, \gamma_3$ from the upper part of the figure are shown. While γ_1 and γ_2 are only represented by one arc each, the geodesic γ_3 appears as two arcs in the fundamental domain.

the sequel (in all proofs it is more convenient to do the calculations from the algebraic point of view). It is however important to realize that the standard Bowen-Series IFS seems to be very natural from the algebraic point of view (it is directly constructed from the two generators S_1, S_2 of the freely generated Schottky group) but not from the point of view of the geodesic flow: Geodesics that turn one time around one of the funnels and which are topologically similar are treated differently depending on the choice of the funnel. For example the geodesics γ_1 and γ_2 in Figure 4.1 only cross one cut line, while the geodesic γ_3 crosses two of them. This implies that γ_3 corresponds to a periodic orbit of word length two while γ_1 and γ_2 only correspond to a word length one. From a purely dynamical point of view it would thus be more natural to take a Poincaré section with three cut lines as presented on the lower part of Figure 4.2. The Schottky surface can then be thought of being obtained by gluing together two identical domains (see Figure 4.2). We will see below that these domains correspond to fundamental domains of a McMullen reflection group .

The aim of this section is thus to construct a holomorphic IFS leading to a dynamical zeta function that also equals the Selberg zeta function but which is constructed in the spirit of Figure 4.2. This *flow-adapted* IFS will turn out to be the natural choice for proving the analyticity of the generalized zeta function (Theorem 1.2) and a crucial ingredient for proving the geometric limits (Theorem 1.3).

The flow-adapted IFS will be obtained by doubling a McMullen reflection IFS [19] (see also [15, Section 6]) and we will first recall the definition of a McMullen reflection group. Those groups are best visualized in the Poincaré disk model. Let c_1, c_2, c_3 denote three geodesics that do not intersect. Geometrically these geodesics are circles that are perpendicular to the disk boundary $\partial\mathbb{D}$ (see upper part of Figure 4.2). The reflection at the geodesic c_i is then an antiholomorphic isometry

$$\rho_{c_i}(u) : \mathbb{D} \rightarrow \mathbb{D}$$

and the Kleinian group Γ generated by the reflections ρ_{c_i} is called a McMullen reflection group. Note that it contains as well orientation preserving (i.e. holomorphic) as orientation inverting (i.e. antiholomorphic) isometries. The subgroup Γ^+ of orientation preserving isometries is then a Schottky group of a 3-funneled surface containing only hyperbolic transformations. If we introduce the displacement length of an hyperbolic positive isometry T as

$$l(T) := \min_{u \in \mathbb{D}} \text{dist}_{\mathbb{D}}(u, Tu),$$

then we can always construct a McMullen reflection group with the following properties.

Lemma 4.1. *Let $l_1, l_2, l_3 > 0$ be real positive numbers, then there exist non-intersecting geodesics c_A, c_B, c_C such that $\rho_{c_A}, \rho_{c_B}, \rho_{c_C}$ generate a McMullen reflection group and the displacement length of the composition of two different generators is given by*

$$l(\rho_{c_B}\rho_{c_C}) = l_1, \quad l(\rho_{c_A}\rho_{c_C}) = l_2, \quad l(\rho_{c_A}\rho_{c_B}) = l_3. \quad (4.1)$$

Proof. First we use the fact from hyperbolic trigonometry (see e.g. [3, Lemma 13.2]) that given three positive numbers α, β, γ there exist positive numbers A, B, C and

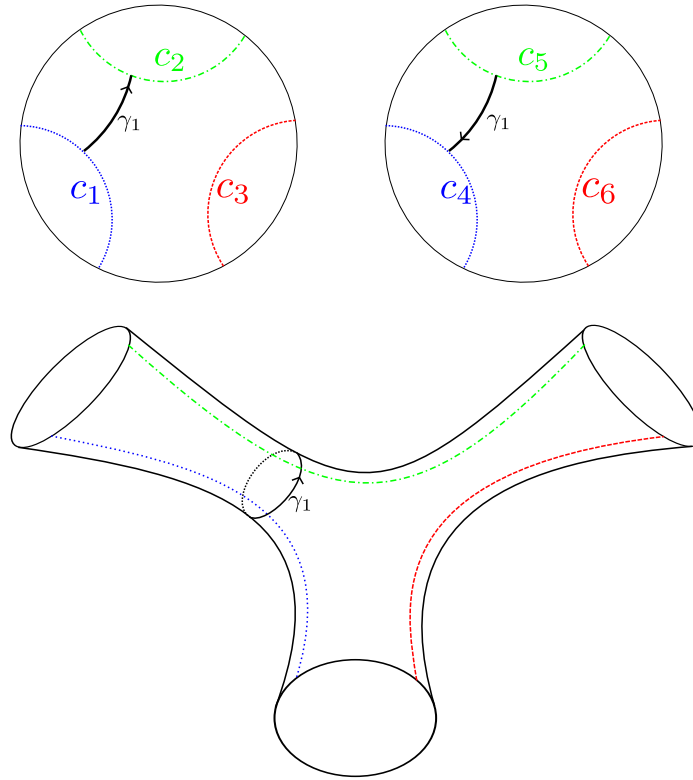


Figure 4.2: Lower part: Schematic sketch of a 3-funneled Schottky surface. The red, green and blue lines indicate the cut lines which would correspond to the Poincaré section of the flow-adapted IFS. The black line γ_1 represents a geodesic which winds once around one of the funnels. Upper part: Fundamental domain of two McMullen IFS represented in the Poincaré disk \mathbb{D} . The Schottky surface below can be obtained by gluing those two fundamental domains together along the cycles such that the colors match each other. In black the two arcs of the geodesic γ_1 are sketched.

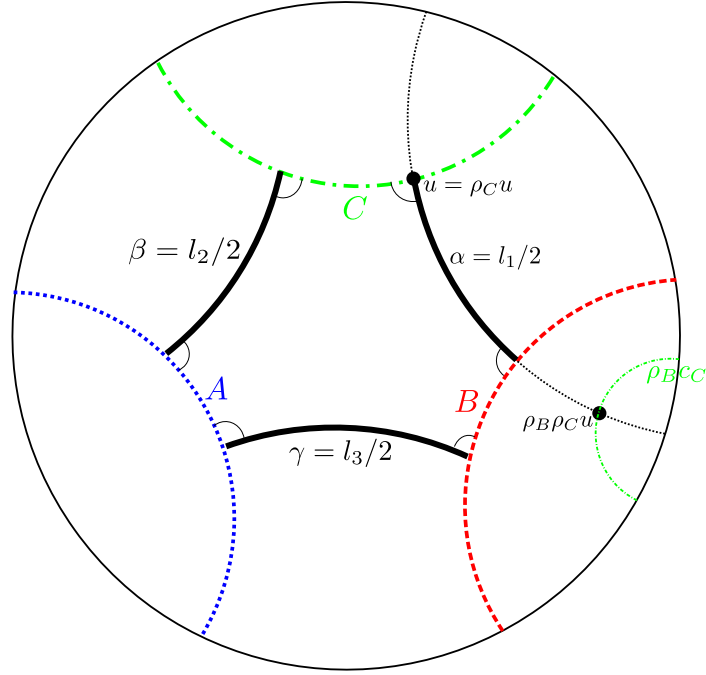


Figure 4.3: Sketch of the orthogonal hexagon in the Poincaré disk \mathbb{D} together with the notations from the proof of Lemma 4.1.

a right-angled hexagon with side lengths $\alpha, C, \beta, A, \gamma, B$ (see Figure 4.3). Note that the geodesic lines c_A, c_B, c_C obtained as the prolongation of A, B, C do not intersect as they are perpendicular to a common geodesic. Thus the reflections along these three geodesics generate a McMullen reflection group. If we choose $\alpha = l_1/2, \beta = l_2/2, \gamma = l_3/2$ we also have (4.1) which can be seen as follows. Let c_α be the geodesic prolongation of the side α . As it is perpendicular to c_B and c_C it is preserved under the reflection along both circles and is thus also preserved under the hyperbolic element $\rho_{c_B}\rho_{c_C}$. Such an invariant geodesic of a hyperbolic element is also called *axis* and it is known that the displacement length is given for any $u \in c_\alpha$ by (see e.g. [3, Section 2.1])

$$l(\rho_{c_B}\rho_{c_C}) = d_{\mathbb{D}}(u, \rho_{c_B}\rho_{c_C}u).$$

Choosing u to be the intersection point of c_C and c_α one immediately sees that

$$d_{\mathbb{D}}(u, \rho_{c_B}\rho_{c_C}u) = d_{\mathbb{D}}(u, \rho_{c_B}u) = 2\alpha = l_1.$$

□

The flow-adapted IFS of a Schottky surface X_{l_1, l_2, l_3} will be constructed from the

generators $\rho_{c_A}, \rho_{c_B}, \rho_{c_C}$. It is however convenient to transform them by the isometry

$$C : \begin{cases} \mathbb{D} & \rightarrow & \mathbb{H} \\ u & \mapsto & -i \frac{u-1}{u+1} \end{cases} \quad (4.2)$$

to the upper half plane. Without loss of generality we can assume that the boundary point $-1 \in \partial\mathbb{D}$ is not contained in any of the disks bounded by c_A, c_B, c_C . The transformation thus gives us 6 points $a_1 < b_1 < a_2 < b_2 < a_3 < b_3 \in \mathbb{R} = \partial\mathbb{H}$ and three geodesic circles c_i with start- and end-points a_i and b_i (see Figure 4.4 for an illustration). If we denote by m_i the center and by r_i the radius of the circle c_i then the reflection at this geodesic is given by

$$\rho_{c_i}(u) = \frac{r}{\bar{u} - m_i} + m_i$$

which is an antiholomorphic map on \mathbb{H} . For holomorphic IFS we however need holomorphic maps on \mathbb{C} , so we extend the map antiholomorphically to \mathbb{C} and compose it with a complex conjugation which gives a holomorphic transformation on \mathbb{C} given by

$$R_i(u) = \frac{r_i}{u - m_i} + m_i. \quad (4.3)$$

which can also be expressed as a Moebius transformation with the matrix

$$R_i = \frac{1}{\sqrt{r_i}} \begin{pmatrix} m_i & r_i - m_i^2 \\ 1 & m_i \end{pmatrix}, \quad (4.4)$$

Note that $\det R_i = -1$ thus the matrices R_i are not in $SL(2, \mathbb{R})$ but any product of an even number of R_i is. Finally, by choosing the indices appropriately, equation (4.1) transforms to

$$l(R_1 R_2) = l_1, \quad l(R_2 R_3) = l_2, \quad l(R_1 R_3) = l_3. \quad (4.5)$$

We can now define the flow-adapted IFS.

Definition 4.2 (Flow-adapted IFS). Let l_1, l_2, l_3 be real positive numbers and let c_i, a_i, b_i, m_i, r_i and R_i be constructed as above from Lemma 4.1. We define the offset variable

$$\delta_{\text{offset}} := b_3 - a_1 + 1.$$

The *flow-adapted IFS* then is a holomorphic IFS with $N = 6$ where the disks D_i are the Euclidean disks in \mathbb{C} with centers m_i and radii r_i for $1 \leq i \leq 3$ and with centers $m_{i-3} + \delta_{\text{offset}}$ and radii r_{i-3} for $4 \leq i \leq 6$. The adjacency matrix A is given by $A_{i,j+3} = A_{j+3,i} = 1$ for all $1 \leq i, j \leq 3$ with $i \neq j$ and $A_{i,j} = 0$ else. Finally for $i \rightsquigarrow j$ the maps $\phi_{i,j}$ are given by

$$\phi_{i,j}(u) := \begin{cases} R_{j-3}(u) + \delta_{\text{offset}} & \text{for } i \leq 3 \\ R_j(u - \delta_{\text{offset}}) & \text{for } i > 3. \end{cases}$$

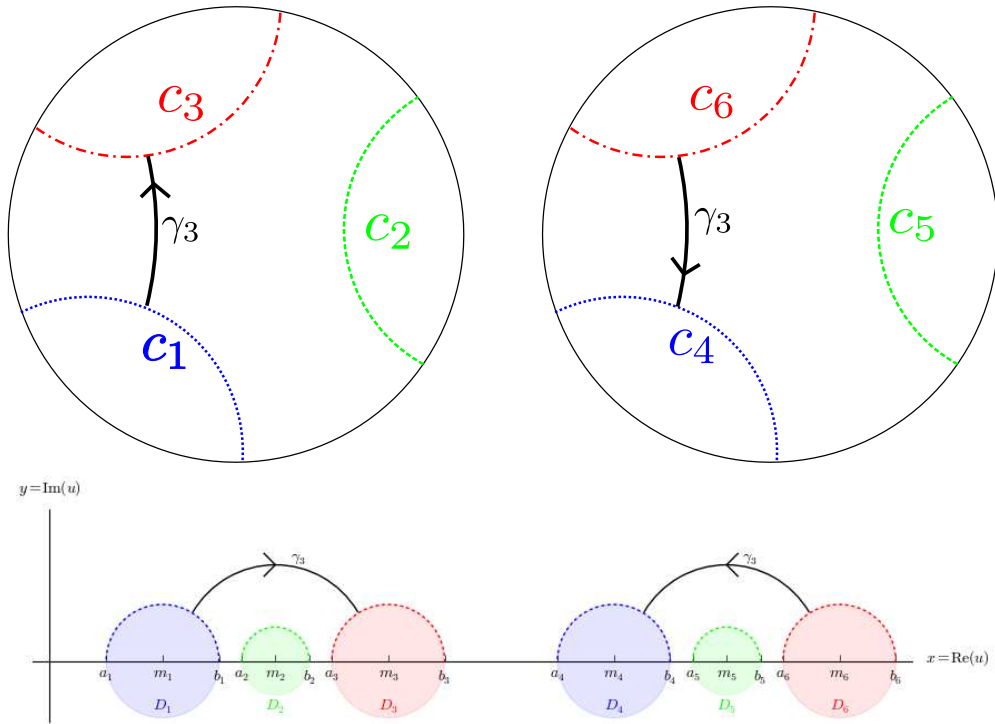


Figure 4.4: Upper part: The two copies of the fundamental domain of the McMullen reflection group from Figure 4.2. Lower part: Disk of the associated flow-adapted IFS with the notations as in Definition 4.2.

Remark 4.3. Note that the concrete form of the flow-adapted IFS is far from being uniquely defined by the lengths l_i . The three lengths only determine uniquely the side lengths of the orthogonal hexagon in the proof of Lemma 4.1 but not its orientation and position inside \mathbb{D} . So every other realization of this pentagon where the point -1 is not contained in any of the disks leads to an equivalent IFS. Additionally the offset variable is completely arbitrary, provided it assures that the disks D_i are mutually disjoint.

As indicated in the discussion above, we want to show that the dynamical zeta function of the flow-adapted IFS with a suitable potential also equals the Selberg zeta function. The key ingredient for this equality is, as in the case of the ordinary Bowen-Series map, a one-to-one correspondence between the classes of prime closed words of the IFS and the primitive closed geodesics which we want to state and prove next.

Proposition 4.4. *Let l_1, l_2, l_3 be positive, real numbers and consider the corresponding flow-adapted IFS from Definition 4.2. Then there exists a bijection between the classes of prime words in $[\mathcal{W}^{\text{prime}}]$ and the primitive closed geodesics on X_{l_1, l_2, l_3} . Additionally the length of the geodesic associated to $[w]$ is given by*

$$-\log(\phi'_w(u_w)). \quad (4.6)$$

Proof. Let R_1, R_2, R_3 be as in Definition 4.2 and $\Gamma = \langle R_1, R_2, R_3 \rangle^+$ the subgroup of orientation preserving isometries of the McMullen reflection group. Then Γ is generated by the two hyperbolic isometries $S_1 = R_1 R_2$ and $S_2 = R_2 R_3$ and it is straightforward to check that S_1, S_2 generate the Schottky group Γ_{l_1, l_2, l_3} . Thus it is known (see e.g. [3, Proposition 2.16]) that the set of primitive closed geodesics on X_{l_1, l_2, l_3} is in bijection to the set of primitive conjugacy classes $[T] \in \Gamma$ where primitive means that there is no $S \in [T]$ such that $S = R^k$ for some $R \in \Gamma$ and $k > 1$. Consequently our aim is to construct a bijection

$$T : [\mathcal{W}^{\text{prime}}] \rightarrow \{\text{primitive conjugacy classes of } \Gamma\}.$$

In order to do so, we note that for $w \in \mathcal{W}_k$ from the form of the adjacency matrix in Definition 4.2 we have $w_i \leq 3 \Rightarrow w_{i+1} > 3$. Thus, if w is a closed word, k has to be even. We first define the map

$$T : [\mathcal{W}^{\text{cl}}] \rightarrow \{\text{conjugacy classes of } \Gamma\}.$$

on the closed words and will later show that we can easily restrict it to the prime words. For a closed word $w = (w_0, \dots, w_{2r})$ we define the map T by

$$T(w) := \begin{cases} R_{w_{2r}} R_{w_{2r-1}-3} \dots R_{w_2} R_{w_1-3} & \text{if } w_0 \leq 3 \\ R_{w_{2r-1}} R_{w_{2r-2}-3} \dots R_{w_1} R_{w_0-3} & \text{if } w_0 > 3 \end{cases}.$$

As closed words have to be of even length, $T(w)$ consists of an even number of reflections and is thus a positive isometry. We first show that T is well defined on $[\mathcal{W}^{\text{prime}}]$, i.e. that it doesn't depend on the choice of the representative of $[w]$. So let $v \in [w]$. Without loss of generality we can assume that $w_0 \leq 3$ and $v_0 \leq 3$ because otherwise

we could simply apply the right-shift σ_R to obtain such an element in the same equivalence class that fulfills this condition and that is mapped to the identical element in Γ . Consequently there exists an integer $0 \leq t \leq r$ such that $v = (w_{2t}, \dots, w_{2r}, w_1, \dots, w_{2t})$ and we obtain

$$T(v) = R_{w_{2t}} \dots R_{w_1-3} R_{w_{2r}} \dots R_{w_{2t+2}} R_{w_{2t+1}-3} = S^{-1}T(w)S$$

for $S = R_{w_{2r}} \dots R_{w_{2t+1}-3}$. Thus $T(v)$ is in the same conjugacy class as $T(w)$.

In order to see the injectivity we take two words v and w that are mapped to the same conjugacy class. We assume first that

$$T(v) = R_a R_b T(w) R_b R_a.$$

However from the form of the adjacency matrix, it is not possible that an element in the image of T starts and ends with the same generator. Thus we have either

$$R_b R_a = R_{w_1-3} R_{w_2}$$

or

$$R_a R_b = R_{w_{2r-1}-3} R_{w_{2r}}.$$

In the first case we have $v = \sigma_L^2 w$ in the latter case $v = \sigma_R^2 w$. By iterating this argument for arbitrary conjugations of $T(w)$ and $T(v)$ we have shown the injectivity of the map T .

In order to see the surjectivity, let $S \in \Gamma$ be an arbitrary element. By definition of Γ we can write $S = R_{s_{2r}} \dots R_{s_1}$ with $1 \leq s_i \leq 3$. As two consecutive identical reflections cancel each other we can assume that $s_i \neq s_{i+1}$. Finally while $s_1 = s_{2r}$ we can conjugate S by $R_{s_2} R_{s_1}$ which leads to an element composed from $2r - 2$ reflections. By iterative conjugation we can thus reduce the element to $\tilde{S} = R_{\tilde{s}_{2\bar{r}}} \dots R_{\tilde{s}_1}$ with $\tilde{s}_1 \neq \tilde{s}_{2\bar{r}}$ and we obtain

$$\tilde{S} = T((s_{2\bar{r}}, s_1 + 3, s_2, \dots, s_{2\bar{r}-1} + 3, s_{2\bar{r}})).$$

We have thus constructed a bijective map between the classes of closed words and the conjugacy classes in Γ . We will now prove that this map can be restricted to a bijection between the classes of prime words and the primitive conjugacy classes. As T is a bijection and on both sides an element can either be primitive or composite it suffices to show that T maps composite closed words to composite conjugacy classes. This is, however, straight forward from the definition of T as obviously $T([w^k]) = T([w])^k$.

With this restriction we have constructed a bijection between the classes of closed, prime words and primitive conjugacy classes. Using the above mentioned result on the one-to-one correspondence between oriented primitive geodesics and primitive conjugacy classes, this is equivalently a bijection to the set of primitive, oriented, closed geodesics and it only remains to prove (4.6).

In order to achieve this, we first recall that the length of the primitive geodesic associated to a conjugacy class of an hyperbolic element $T \in \Gamma$ is equal to the displacement length of T (see e.g. [3, Proposition 2.16]) and it is also a well known fact

that if $u_T \in \partial\mathbb{H}$ is the stable fixed point of T then $l(T) = -\log((T)'(u_T))$ (see e.g. [3, (15.2)]). Next we recall from the proof of Theorem 3.5 that $\phi'_w(u_w)$ is independent of the representative in $[w]$. Assuming once more, that $w_0 \leq 3$ we calculate that

$$\phi_w(u_w) = R_{w_{2r}} \dots R_{w_{1-3}} u_w.$$

Thus u_w is the stable fixed point of the hyperbolic element $T(w)$ and for the displacement length of T we obtain $l(T(w)) = -\log((T(w))'(u_w))$. As however the displacement length coincides with the length of the associated closed geodesic (see e.g. [3, Proposition 2.16]) we established (4.6) and finished the proof of Proposition 4.4. \square

Corrolary 4.5. *Let l_1, l_2, l_3 be real positive numbers, and \mathcal{L}_s the Ruelle transfer operator of the flow-adapted IFS as defined in Definition 4.2 with potential $V_s(u) = [(\phi^{-1})'(u)]^{-s}$, then the dynamical zeta function coincides with the Selberg zeta function of X_{l_1, l_2, l_3}*

$$Z_{X_{l_1, l_2, l_3}}(s) = \det(1 - \mathcal{L}_s)$$

Proof. As (3.9) did not depend on the choice of the IFS we obtain also for the flow-adapted IFS

$$\det(1 - \mathcal{L}_s) = \prod_{[w] \in [\mathcal{W}^{\text{prime}}]} \prod_{k \geq 0} (1 - \phi'_w(u_w)^{k+s}).$$

Using Proposition 4.4 this can be written as

$$\det(1 - \mathcal{L}_s) = \prod_{\gamma \in \mathcal{P}_{X_{l_1, l_2, l_3}}} \prod_{k \geq 0} (1 - e^{-(k+s)l(\gamma)}).$$

which is exactly the Selberg zeta function of X_{l_1, l_2, l_3} . \square

With help of the flow-adapted IFS we can now prove the analyticity of the generalized zeta functions which was stated in the introduction as Theorem 1.2.

Theorem 1.2. *Let X_{l_1, l_2, l_3} be a Schottky surface with three funnels of widths l_1, l_2, l_3 and let $n_1, n_2, n_3 \in \mathbb{N}$. We define*

$$\mathbf{n} : \begin{cases} \mathcal{P}_{X_{l_1, l_2, l_3}} & \rightarrow \mathbb{N} \\ \gamma & \mapsto \sum_{i=1}^3 n_i w_i(\gamma) \end{cases}$$

where $w_i(\gamma)$ denotes the winding number around the funnel of width l_i . Then the generalized zeta function

$$d_{\mathbf{n}}(s, z) = \prod_{\gamma \in \mathcal{P}_{X_{l_1, l_2, l_3}}} \prod_{k \geq 0} (1 - z^{\mathbf{n}(\gamma)} e^{-(k+s)l(\gamma)}).$$

extends to an analytic function on \mathbb{C}^2 .

Proof. First we note that for $|z| < 1$ and $\operatorname{Re}(s) > 1$ the products in (1.3) expand to an absolutely convergent series. In the region of absolute convergence we can Taylor expand $d_{\mathbf{n}}$ in z around zero and obtain

$$d_{\mathbf{n}}(s, z) = \sum_{k=0}^{\infty} b_k(s) z^k. \quad (4.7)$$

In order to show the analytic continuation we construct an appropriate s - and z -dependent trace class operator. We take the flow-adapted IFS and define a potential V which depends analytically on two complex parameters $s, z \in \mathbb{C}$ by setting for $i \rightsquigarrow j$ and $u \in \phi_{i,j}(D)$

$$V(u; s, z) := z^{n_{i,j}} [-(\phi^{-1})'(u)]^{-s}$$

where

$$\begin{aligned} n_{1,5} = n_{5,1} = n_{4,2} = n_{2,4} &:= n_1 \\ n_{2,6} = n_{6,2} = n_{5,3} = n_{3,5} &:= n_2 \\ n_{3,4} = n_{4,3} = n_{6,1} = n_{1,6} &:= n_3 \end{aligned}$$

Note that $-(\phi^{-1})'$ is non-vanishing on $\phi(D)$ and real and positive on $\Phi(D) \cap \mathbb{R}$, so we can extend for each $s \in \mathbb{C}$ the function $[-(\phi^{-1})']^{-s}$ from the real line to each of the disks $\phi_{i,j}(D_i)$ and obtain this way a family of holomorphic and bounded potentials on $\phi(D)$ that depends analytically on s and z . Following [15, Proposition 2] the family of transfer operators

$$\mathcal{L}_{s,z} := \mathcal{L}_{V(\bullet; s, z)} \quad (4.8)$$

with this potential is nuclear on $\mathcal{A}_{\infty}(D)$ and as a consequence of the analytic dependence of V on the parameters s, z the Fredholm determinant $\det(1 - \mathcal{L}_{s,z})$ also is an analytic function of s, z . The choice of the factors z^{n_i} is exactly such that each half winding around one of the i -th funnel contributes with a factor z^{n_i} . Thus each winding around the i -th funnel contributes with $2n_i$ and the total dynamical zeta function is in the region of absolute convergence given by

$$\tilde{d}_{\mathbf{n}}(s, z) := \det(1 - \mathcal{L}_{s,z}) = \prod_{\gamma \in \mathcal{P}_{X_{l_1, l_2, l_3}}} \prod_{k \geq 0} \left(1 - z^{2\mathbf{n}(\gamma)} e^{-(k+s)l(\gamma)} \right). \quad (4.9)$$

As we know that the function is analytic we can Taylor expand it in z around 0 and obtain

$$d_{\mathbf{n}}(s, z) = \sum_{k=0}^{\infty} b_k(s) z^k. \quad (4.10)$$

with analytic coefficients $b_k(s)$. As in (4.9) only even powers of z appear we immediately can conclude $b_{2k+1}(s) = 0$. Comparing furthermore the product expressions (1.3) with (4.9) and the Taylor expansions (4.7) with (4.10) in the region of absolute convergence we obtain

$$b_k(s) = \tilde{b}_{2k}(s).$$

By this identification we obtain an analytic continuation of the Taylor coefficients $b_k(s)$. As for each $s \in \mathbb{C}$ the power series (4.10) has a radius of convergence equal to infinity, i.e. $\limsup_k |\tilde{b}_k(s)|^{1/k} = 0$ we also obtain that (4.7) converges for all $z \in \mathbb{C}$ and the generalized zeta function is thus analytic. \square

5 Geometric limits

In this section we will prove Theorem 1.3 and then show that Theorem 1.1 is a consequence of this result. The proof of Theorem 1.3 will be performed in three steps: First we will derive a form of the flow-adapted IFS, that is especially suited to treat the family of Schottky surfaces in the limit $\ell \rightarrow \infty$. In a next step (Lemma 5.2) we will derive explicit bounds for the coefficients of the cycle expansion of the generalized zeta function. Finally we will be able to prove the convergence using these bounds and the special form of the flow-adapted IFS (See Lemma 5.6 and 5.7 as well as the rest of this section).

We start with the construction of the special form of flow-adapted IFS.

Lemma 5.1. *Let n_1, n_2, n_3 be positive integers fulfilling the triangle condition. Then there exists ℓ_0 such that for any $\ell > \ell_0$ there exists a family of flow-adapted IFS associated to $X_{n_1, n_2, n_3}(\ell)$ in the sense of Definition 4.2 such that the lower boundaries a_j of the disks D_j are given by $a_j = 2(j-1)$ independently of ℓ and $r_j < 0.5$. Furthermore the radii fulfill the asymptotics*

$$\lim_{\ell \rightarrow \infty} r_j(\ell) e^{\kappa_j \ell} = C_j \quad (5.1)$$

where

$$\kappa_1 = \frac{n_1 + n_3 - n_2}{2}, \quad \kappa_2 = \frac{n_1 + n_2 - n_3}{2}, \quad \kappa_3 = \frac{n_2 + n_3 - n_1}{2}$$

and $\kappa_4 = \kappa_1, \kappa_5 = \kappa_2, \kappa_6 = \kappa_3$ are constants strictly larger than zero and

$$C_1 = C_3 = C_4 = C_6 = 8, \quad C_2 = C_5 = \frac{1}{2}.$$

Proof. We will first use the freedom of choosing the position and orientation of the hexagon as already mentioned in Remark 4.3. Instead of constructing the reflection group on \mathbb{D} we can also directly work on the upper half plane (see Figure 5.1). So we can consider again an orthogonal hexagon with side lengths $A, n_1\ell/2, B, n_2\ell/2, C, n_3\ell/2$ and we call c_1 to be the geodesic prolongation of the side A , c_2 the one of B and c_3 the one of C . Now there exists an isometry such that for the starting points $a_j \in \mathbb{R} = \partial\mathbb{H}$ of c_j we have $a_j = 2j$. This isometry can be constructed in three steps: First translate parallel to the real axis until $a_1 = 0$, then apply the dilation $z \rightarrow \lambda z$ which fixes a_1 until $a_2 = 2$ and finally apply the one parameter group of hyperbolic transformation that fixes a_1, a_2 until $a_3 = 6$ is fulfilled. Setting the offset parameter $\delta_{\text{offset}} = 6$ we then obtain the condition $a_j = 2(j-1)$ for all $1 \leq j \leq 6$. Note however that the flow-adapted IFS might be ill defined with this offset parameter, because we could in

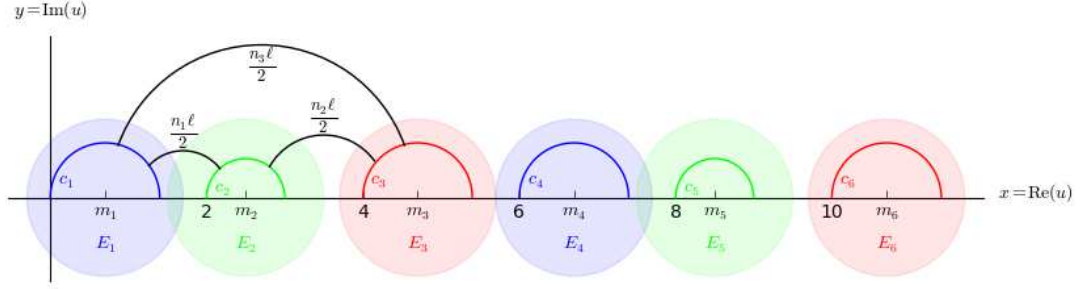


Figure 5.1: Illustration of the construction of the family of flow-adapted IFS in Lemma 5.1. The start points of the circles c_j are now fixed to $2(j - 1)$. The light colored disks indicate the extended disks E_j which are crucial for obtaining the estimates in Lemma 5.2.

principle have $r_3 > 1$. In the next step we will show however that in the limit $\ell \rightarrow \infty$ all radii r_j will tend to zero. Thus for sufficiently large ℓ everything is well defined.

In order to show the convergence of the radii to zero we first note that even without the triangle condition at least two of the radii have to converge towards zero. Otherwise the perpendicular distance between those two circles can never tend towards infinity as already the distance between their start points a_i is fixed. We can thus assume, after possibly permuting the l_i that r_1 and r_3 converge to zero. For a proof by contradiction we now assume that r_2 is bounded away from zero by r_{\min} . We will first show that then also the side length B is bounded away from zero: For $x \in \partial\mathbb{H}$ and $r > 0$ we consider the unique geodesic that starts in x and is orthogonal to the circle of radius r that starts at a_2 . We denote the intersection point of these two geodesics with $p(x, r)$. Then for two different points $x_1 \neq x_2$ the points $p(x_1, r)$ and $p(x_2, r)$ are different. Recall that B is exactly the hyperbolic distance between $p(r_2, x_1)$ and $p(r_2, x_2)$ where $x_1 \in [a_1, a_1 + 2r_1]$ and $x_2 \in [a_3, a_3 + 2r_3]$ such that the geodesics are also orthogonal to c_1 and c_3 , respectively (see Figure 5.2 for an illustration of these points). From the fact that the disks D_i are mutually disjoint we conclude, that $[a_1, a_1 + 2r_1] \cap [a_3, a_3 + 2r_3] = \emptyset$ so $d_{\mathbb{H}}(p(x_1, r_2), p(x_2, r_2)) > 0$ for all ℓ . Furthermore the disjoint disk and the lower bound on r_2 together imply that $r_2 \in [r_{\min}, 1]$. The fact that r_1 and r_2 converge to zero finally means that there exist $r_{1, \max}, r_{3, \max}$ such that $r_1 \leq r_{1, \max}$ and $r_3 \leq r_{3, \max}$ for all ℓ . We can thus bound

$$B = d_{\mathbb{H}}(p(x_1, r_2), p(x_2, r_2)) \geq \min_{\substack{y_1 \in [a_1, a_1 + 2r_{1, \max}], \\ y_2 \in [a_3, a_3 + 2r_{3, \max}], \\ r \in [r_{\min}, 1]}} d_{\mathbb{H}}(p(y_1, r), p(y_2, r)) =: B_0.$$

As $d_{\mathbb{H}}(p(y_1, r), p(y_2, r))$ is a positive quantity that depends continuously on the parameters r, y_1, y_2 which vary in a compact set, $B_0 > 0$ and B is bounded away from zero. This is however in contradiction to the triangle condition. From [29, (2.6.10)]

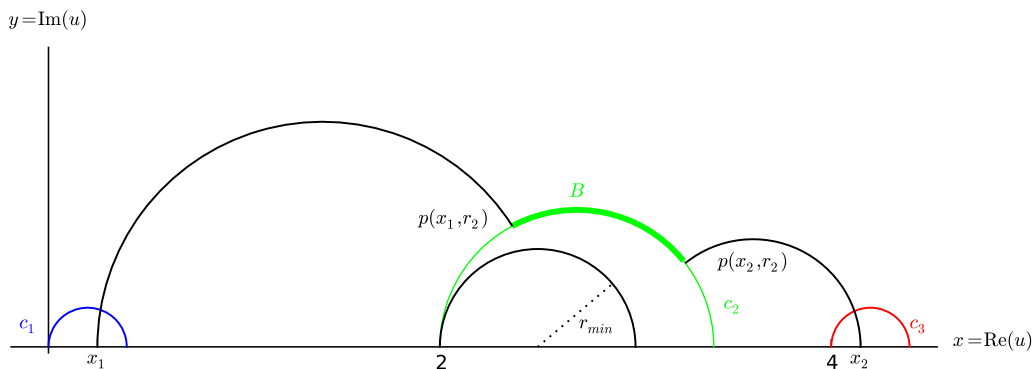


Figure 5.2: Illustration of the notation for the lower bound on B in the proof of Lemma 5.1.

we have the formula for orthogonal hexagons

$$\cosh B = \frac{\cosh(n_1\ell/2) \cosh(n_2\ell/2) + \cosh(n_3\ell/2)}{\sinh(n_1\ell/2) \sinh(n_2\ell/3)}.$$

In the limit $\ell \rightarrow \infty$ the right side becomes

$$1 + \frac{e^{n_3\ell}}{e^{(n_1+n_2)\ell}}$$

which converges to 1 if the triangle condition is fulfilled and consequently $\lim_{\ell \rightarrow \infty} B = 0$. We have thus shown that under the triangle condition all three radii have to converge to zero.

In order to prove the concrete form of the asymptotics (5.1) we use the following general formula for the displacement length of an hyperbolic element $T \in SL(2, \mathbb{R})$

$$\cosh(l(T)/2) = |\text{Tr}(T)/2|.$$

So using (4.5) together with the explicit form (4.4) for the R_i one obtains the set of equations.

$$\begin{aligned} \cosh(n_1\ell/2) = \cosh(l(R_1R_2)/2) &= \left| \frac{\text{Tr}(R_1R_2)}{2} \right| = \frac{(m_1 - m_2)^2 - r_1 - r_2}{2\sqrt{r_1r_2}} \\ \cosh(n_2\ell/2) = \cosh(l(R_2R_3)/2) &= \left| \frac{\text{Tr}(R_2R_3)}{2} \right| = \frac{(m_2 - m_3)^2 - r_2 - r_3}{2\sqrt{r_2r_3}} \\ \cosh(n_3\ell/2) = \cosh(l(R_1R_3)/2) &= \left| \frac{\text{Tr}(R_1R_3)}{2} \right| = \frac{(m_1 - m_3)^2 - r_1 - r_3}{2\sqrt{r_1r_3}}. \end{aligned}$$

Dividing both sides by $e^{n_i \ell/2}$ and taking the limit $\ell \rightarrow \infty$ one obtains

$$\begin{aligned} 1 &= \lim_{\ell \rightarrow \infty} \frac{\cosh n_1 \ell/2}{e^{n_1 \ell/2}} = \lim_{\ell \rightarrow \infty} \frac{(m_1 - m_2)^2 - r_1 - r_2}{2\sqrt{r_1 r_2} e^{n_1 \ell/2}} \\ 1 &= \lim_{\ell \rightarrow \infty} \frac{\cosh n_2 \ell/2}{e^{n_1 \ell/2}} = \lim_{\ell \rightarrow \infty} \frac{(m_2 - m_3)^2 - r_2 - r_3}{2\sqrt{r_2 r_3} e^{n_2 \ell/2}} \\ 1 &= \lim_{\ell \rightarrow \infty} \frac{\cosh n_3 \ell/2}{e^{n_3 \ell/2}} = \lim_{\ell \rightarrow \infty} \frac{(m_1 - m_3)^2 - r_1 - r_3}{2\sqrt{r_1 r_3} e^{n_3 \ell/2}}. \end{aligned}$$

From the fact that the a_i do not depend on ℓ and that the radii all converge to zero we explicitly know $\lim_{\ell \rightarrow \infty} (m_i - m_j)^2 - r_i - r_j$ and obtain

$$\begin{aligned} \lim_{\ell \rightarrow \infty} \sqrt{r_1 r_2} e^{n_1 \ell/2} &= 2 \\ \lim_{\ell \rightarrow \infty} \sqrt{r_2 r_3} e^{n_2 \ell/2} &= 2 \\ \lim_{\ell \rightarrow \infty} \sqrt{r_1 r_3} e^{n_3 \ell/2} &= 8. \end{aligned}$$

We now multiply two of these equations and divide by the third one and obtain

$$\begin{aligned} \lim_{\ell \rightarrow \infty} r_1 e^{(n_1 + n_3 - n_2) \ell/2} &= 8 \\ \lim_{\ell \rightarrow \infty} r_2 e^{(n_1 + n_2 - n_3) \ell/2} &= \frac{1}{2} \\ \lim_{\ell \rightarrow \infty} r_3 e^{(n_2 + n_3 - n_1) \ell/2} &= 8 \end{aligned}$$

which finishes the proof of Lemma 5.1. \square

From the property $r_j < 0.5$ of these flow-adapted IFS it directly follows that for any $\ell > \ell_0$ and any $1 \leq j \leq 6$ there exists extended disks E_j which are concentric with D_j , have a radius $r_{E_j} > 1$ and do not intersect any of the other disks D_i (see Figure 5.1 for an illustration).

Lemma 5.2. *Let n_1, n_2, n_3 be positive integers fulfilling the triangle condition and $\ell > \ell_0$ as in Lemma 5.1. Let $d_{\mathbf{n}}(s, z)$ be the generalized zeta function of the family of Schottky surfaces $X_{n_1, n_2, n_3}(\ell)$. Let furthermore $\mathcal{L}_{s, z; \ell}$ be the transfer operator as defined in (4.8) of the flow-adapted IFS from Lemma 5.1 and let its cycle expansion be given by*

$$\det(1 - y \mathcal{L}_{s, z; \ell}) = 1 + \sum_{k=1}^{\infty} y^k \tilde{d}_{\mathbf{n}}^{(k)}(s, z; \ell). \quad (5.2)$$

With this definition of $\tilde{d}_{\mathbf{n}}^{(k)}(s, z; \ell)$ we can express the generalized zeta function as

$$d_{\mathbf{n}}(s, z; \ell) = 1 + \sum_{k=1}^{\infty} \tilde{d}_{\mathbf{n}}^{(k)}(s, \sqrt{z}; \ell). \quad (5.3)$$

If we furthermore fix six disks E_j with radius $r_{E_j} > 1$ and center m_j such that for $i \neq j$ $E_i \cap D_j = \emptyset$ then we have the explicit bounds

$$|\tilde{d}_{\mathbf{n}}^{(k)}(s, z; \ell)| \leq k^{k/2} K(s, z; \ell)^k \sum_{m_1 < \dots < m_k} r(\ell)^{\lfloor m_1/6 \rfloor + \dots + \lfloor m_k/6 \rfloor}, \quad (5.4)$$

where $\lfloor x \rfloor$ denotes the integer part of a real number x and

$$r(\ell) := \max_{1 \leq j \leq 6} r_j \quad \text{and} \quad K(s, z; \ell) := \frac{1}{2\pi} \max_{j \rightsquigarrow i} \|V(\phi_{j,i}(\bullet); s, z)\|_{\infty, E_j}. \quad (5.5)$$

Remark 5.3. We will follow closely the techniques of Jenkinson-Pollicott [15] which they used to obtain rigorous dimension estimates, but in a different spirit. While they were interested in the question how fast the cycle expansion coefficients $d^{(k)}$ for a fixed IFS vanish if the order k becomes large, we consider the coefficients for a family of IFS at a fixed order k and we want to determine which coefficients vanish in the limit $\ell \rightarrow \infty$. The estimate (5.4) then says that only the first six coefficients survive in this limit.

Proof. We know that the transfer operator $\mathcal{L}_{s,z;\ell}$ of the flow-adapted IFS is a nuclear operator, so using the following result of Grothendieck we obtain a direct formula for the coefficients of the cycle expansion in terms of the nuclear representation.

Proposition 5.4 (Grothendieck 1956 [11]). *If \mathcal{B} is a Banach space and $\mathcal{L} : \mathcal{B} \rightarrow \mathcal{B}$ is a nuclear operator with the nuclear representation $\mathcal{L}h = \sum_{n=1}^{\infty} \lambda_n \alpha_n(h) v_n$ as defined in Definition 3.4, then the Fredholm determinant of \mathcal{L} can be expanded in a power series $\det(1 - z\mathcal{L}) = 1 + \sum_{k=1}^{\infty} z^k d^{(k)}$ with*

$$d^{(k)} = (-1)^k \sum_{m_1 < \dots < m_k} \lambda_{m_1} \dots \lambda_{m_k} \det [(\alpha_{m_p}(v_{m_q}))_{p,q=1}^k] \quad (5.6)$$

where

$$(\alpha_{m_p}(v_{m_q}))_{p,q=1}^k = \begin{pmatrix} \alpha_{m_1}(v_{m_1}) & \dots & \alpha_{m_k}(v_{m_1}) \\ \vdots & \ddots & \vdots \\ \alpha_{m_1}(v_{m_k}) & \dots & \alpha_{m_k}(v_{m_k}) \end{pmatrix}$$

is a $k \times k$ matrix.

Thus (5.6) allows us to obtain estimates on the coefficients $\tilde{d}_{\mathbf{n}}^{(k)}(s, z; \ell)$ in terms of the nuclear representation of $\mathcal{L}_{s,z;\ell}$. We therefore want to derive its nuclear decomposition now and obtain explicit estimates on the λ_n .

Recall from (3.3) that $\mathcal{L}_{s,z;\ell}$ can be decomposed into a sum of the following six operators

$$\left(\mathcal{L}^{(j)} h\right)(u) = \sum_{i \text{ s.t. } j \rightsquigarrow i} V(\phi_{j,i}(u)) h(\phi_{j,i}(u)).$$

with $1 \leq j \leq 6$.

It is now an important remark that the function $\mathcal{L}_{s,z;\ell}^{(j)}h$ is not only holomorphic on D_j but can be extended holomorphically to a much larger disk with the same center. We illustrate the mechanism for $\mathcal{L}_{s,z;\ell}^{(1)}h$ which is given by

$$\begin{aligned} (\mathcal{L}_{s,z;\ell}^{(1)}h)(u) &= V(\phi_{1,5}(u); s, z)h(\phi_{1,5}(u)) + V(\phi_{1,6}(u); s, z)h(\phi_{1,6}(u)) \\ &= z^{n_1} [-R'_2(u)]^s h(R_2(u) + \delta_{\text{offset}}) + z^{n_3} [-R'_3(u)]^s h(R_3(u) + \delta_{\text{offset}}). \end{aligned}$$

The factor $h(R_2(\bullet) + \delta_{\text{offset}})$ is just the pullback of h with a reflection at the boundary of disk D_2 plus complex conjugation and a final translation. Thus from the fact that h is holomorphic on D_5 follows that $h(R_2(\bullet) + \delta_{\text{offset}})$ is holomorphic on $\mathbb{C} \setminus D_2$. For the same reason the term $h(R_3(\bullet) + \delta_{\text{offset}})$ is holomorphic on $\mathbb{C} \setminus D_3$. Let us next consider the term $[-R'_2(u)]^s$. From the form (4.3) one deduces directly that $-R'_2(\bullet)$ is a nonzero holomorphic function on $\mathbb{C} \setminus \{m_2\}$, consequently $[-R'_2(u)]^s$ can be extended to every split plane $\mathbb{C} \setminus l$ where l is a half line starting at the center m_2 and going to infinity. Analogously $[-R'_3]^s$ can be extended to every split plane without a line starting at m_3 . We can therefore extend $\mathcal{L}_{s,z;\ell}^{(1)}h$ to any disk centered around m_1 that does not intersect D_2 nor D_3 and in particular to the disk E_1 as defined above. Analogously any of the other functions $\mathcal{L}_{s,z;\ell}^{(j)}h$ can be extended from D_j to E_j . This extension will now allow us to construct a nuclear representation of the operators $\mathcal{L}_{s,z;\ell}^{(j)}$ and control the appearing terms.

Let us denote by C_j the circle of radius 1 around m_j . As C_j is strictly contained in E_j we can write with the holomorphic extension to E_j and Cauchy's integral formula for any $\ell > \ell_0$ and any $u \in D_j$

$$(\mathcal{L}_{s,z;\ell}^{(j)}h)(u) = \frac{1}{2\pi i} \int_{C_j} \frac{(\mathcal{L}_{s,z;\ell}^{(j)}h)(\xi)}{\xi - u} d\xi.$$

As we know for any $\xi \in C_j$ and $u \in D_j$ that $|u - m_j| < |\xi - m_j|$ we can use the geometric series to write

$$\begin{aligned} (\mathcal{L}_{s,z;\ell}^{(j)}h)(u) &= \frac{1}{2\pi i} \int_{C_j} \frac{(\mathcal{L}_{s,z;\ell}^{(j)}h)(\xi)}{\xi - m_j} \left(1 - \frac{u - m_j}{\xi - m_j}\right)^{-1} d\xi \\ &= \sum_{n=0}^{\infty} \frac{1}{2\pi i} \int_{C_j} \frac{(\mathcal{L}_{s,z;\ell}^{(j)}h)(\xi)}{\xi - m_j} \left(\frac{u - m_j}{\xi - m_j}\right)^n d\xi \\ &= \sum_{n=0}^{\infty} \tilde{\alpha}_n^{(j)}(h) \tilde{v}_n^{(j)}(u), \end{aligned}$$

where

$$\tilde{\alpha}_n^{(j)}(h) := \frac{1}{2\pi i} \int_{C_j} \frac{(\mathcal{L}_{s,z;\ell}^{(j)}h)(\xi)}{(\xi - m_j)^{n+1}} d\xi \quad \text{and} \quad \tilde{v}_n^{(j)}(u) = (u - m_j)^n. \quad (5.7)$$

We can finally normalize the elements $\tilde{v}_n^{(j)}$ with respect to the supremum norm and $\tilde{\alpha}_n^{(j)}$ with respect to the operator norm as a linear operator $\mathcal{A}(D) \rightarrow \mathbb{C}$ and we obtain the nuclear representation

$$(\mathcal{L}_{s,z;\ell}^{(j)} h)(u) = \sum_{n=0}^{\infty} \lambda_n^{(j)} \alpha_n^{(j)}(h) v_n^{(j)}(u)$$

with $\lambda_n^{(j)} = \|\tilde{\alpha}_n^{(j)}\| \|\tilde{v}_n^{(j)}\|$.

Equation (5.7) also allows us to obtain estimates on $\lambda_n^{(j)}$. Recall that r_j was the radius of disk D_j so we have

$$\|\tilde{v}_n^{(j)}\|_{\infty, D_j} = r_j^n.$$

In order to bound $\|\tilde{\alpha}_n^{(j)}\|$ first calculate for any $h \in \mathcal{A}_{\infty}$ that

$$|\tilde{\alpha}_n^{(j)}(h)| \leq \frac{1}{2\pi} \|\mathcal{L}_{s,z;\ell}^{(j)} h\|_{\infty, E_j} \leq \frac{1}{2\pi} \max_{i: j \rightsquigarrow i} \|V(\phi_{j,i}(\bullet); s, z)\|_{\infty, E_j} \|h\|_{\infty, D}$$

so putting the two bounds together we get

$$\begin{aligned} \lambda_n^{(j)} &= \|\alpha_n^{(j)}\| \|\tilde{v}_n^{(j)}\| \\ &\leq r_j^n \frac{1}{2\pi} \max_{i: j \rightsquigarrow i} \|V(\phi_{j,i}(\bullet); s, z)\|_{\infty, E_j}. \end{aligned} \quad (5.8)$$

We have thus derived the nuclear representation of $\mathcal{L}_{s,z;\ell}^{(j)}$ and also obtained explicit bounds on the $\lambda_n^{(j)}$. In order to control the nuclear representation of the full operator $\mathcal{L}_{s,z;\ell}$ we have to sum up the six operators $\mathcal{L}_{s,z;\ell}^{(j)}$ with $1 \leq j \leq 6$. We arrange the different summands such that

$$\mathcal{L}_{s,z;\ell} h = \sum_{n=0}^{\infty} \lambda_n \alpha_n(h) v_n$$

with

$$\lambda_{6n+j} = \lambda_n^{(j)}, \quad \alpha_{6n+j} = \alpha_n^{(j)} \text{ and } v_{6n+j} = v_n^{(j)}.$$

If we define

$$r(\ell) := \max_j (r_j) \text{ and } K(s, z; \ell) := \frac{1}{2\pi} \max_{j \rightsquigarrow i} \|V(\phi_{j,i}(\bullet); s, z)\|_{\infty, E_j}$$

then we have the explicit bound

$$\lambda_n \leq K(s, z; \ell) r(\ell)^{\lfloor n/6 \rfloor}. \quad (5.9)$$

We can now use the Grothendieck formula (5.6) as well as the Hadamard bound on the $k \times k$ matrices with entries lower or equal to one and obtain

$$\begin{aligned} |\tilde{d}_{\mathbf{n}}^{(k)}(s, z, \ell)| &= \sum_{m_1 < \dots < m_k} \lambda_{m_1} \dots \lambda_{m_k} \det [(\alpha_{m_p}(v_{m_q}))_{p,q=1}^k] \\ &\leq k^{k/2} K(s, z; \ell)^k \sum_{m_1 < \dots < m_k} r(\ell)^{\lfloor m_1/6 \rfloor + \dots + \lfloor m_k/6 \rfloor} \end{aligned}$$

which finishes the proof of Lemma 5.2. \square

For the rest of the proof of Theorem 1.3 there remain two steps to be done: First we will show that the bounds in Lemma 5.2 allow to uniformly truncate the cycle expansion after the sixth order and secondly we will show that the finitely many remaining terms converge against the polynomial. For both steps, the following lemma will be useful.

Lemma 5.5. *For any $j \rightsquigarrow i$ and any bounded domain $B \subset \mathbb{C}^2$ we have*

$$\lim_{\ell \rightarrow \infty} V(\phi_{j,i}(u), s/\ell, \sqrt{z}) = z^{n_{j,i}/2} e^{-\kappa_i s}$$

uniformly for $u \in E_i$ and $(s, z) \in B$.

Proof. Recall that

$$V(\phi_{j,i}(u); s/\ell, \sqrt{z}) = z^{n_{j,i}/2} [-(\phi_{j,i}^{-1})'(\phi_{j,i}(u))]^{s/\ell} = z^{n_{j,i}/2} [-\phi'_{j,i}(u)]^{s/\ell}$$

and calculate that for $1 \leq i \leq 3$

$$-\phi'_{j,i}(u) = \frac{r_i}{(u - \delta_{\text{offset}} - m_i)^2}$$

while for $4 \leq i \leq 6$

$$-\phi'_{j,i}(u) = \frac{r_{i-3}}{(u - m_{i-3})^2}.$$

By the definition of the family of flow-adapted IFS in Lemma 5.1 and the extended disks E_i we know that there exist two constants $0 < c < C$ such that for any $j \rightsquigarrow i$, any $u \in E_j$ we have $c < |u - \delta_{\text{offset}} - m_i| < C$ if $i \leq 3$ and $c < |u - m_{i-3}| < C$ if $i > 3$. Furthermore the asymptotics (5.1) for r_i gives us another pair of constants $0 < c < C$ with $c < r_i e^{\kappa_i \ell} < C$. Together with the fact that s can vary only in a bounded set $\text{Pr}_s B$, which is the projection of B to the s variable, this gives the existence of constants $0 < c < C$ with

$$c < (-\phi'_{j,i}(u) e^{\kappa_i \ell})^s < C \quad \forall u \in E_j, \ell > \ell_0 \text{ and } s \in \text{Pr}_s B. \quad (5.10)$$

In order to use this inequality we calculate

$$\begin{aligned} \left\| V(\phi_{j,i}(u), s/\ell, \sqrt{z}) - z^{n_{j,i}/2} e^{-\kappa_i s} \right\|_{\infty, E_j \times B} &= \left\| z^{n_{j,i}/2} \left((-\phi'_{j,i}(u))^{s/\ell} - e^{-\kappa_i s} \right) \right\|_{\infty, E_j \times B} \\ &\leq \left\| z^{n_{j,i}/2} e^{-\kappa_i s} \right\|_{\infty, B} \left\| \left((-\phi'_{j,i}(u) e^{\kappa_i \ell})^{s/\ell} - 1 \right) \right\|_{\infty, E_j \times B}. \end{aligned}$$

While the first term $\left\| z^{n_{j,i}/2} e^{-\kappa_i s} \right\|_{\infty, B}$ is bounded and independent of ℓ , the uniform bounds (5.10) imply that the second term converges to zero. \square

Lemma 5.6. *Let $B \subset \mathbb{C}^2$ be any bounded domain, and*

$$d_{\mathbf{n}}(s, z; \ell) = 1 + \sum_{k=1}^{\infty} \tilde{d}_{\mathbf{n}}^{(k)}(s, \sqrt{z}; \ell).$$

the series expansion (5.3) of the generalized zeta function from Lemma 5.2. Then

$$\lim_{\ell \rightarrow \infty} \left\| \sum_{k>6} \tilde{d}_{\mathbf{n}}^{(k)}(s/\ell, \sqrt{z}; \ell) \right\|_{\infty, B} = 0, \quad (5.11)$$

i.e. the rescaled generalized zeta function $d_{\mathbf{n}}(s/\ell, z; \ell)$ converges uniformly to the finitely truncated sum $1 + \sum_{k=1}^6 \tilde{d}_{\mathbf{n}}^{(k)}(s/\ell, \sqrt{z}; \ell)$.

Proof. In a first step we show that Lemma 5.5 implies a bound for $\|K(s/\ell, \sqrt{z}, \ell)\|_{\infty, B}$. Recall from the definition (5.5) that

$$\|K(s/\ell, \sqrt{z}, \ell)\|_{\infty, B} = \max_{j \rightsquigarrow i} \|V(\phi_{j,i}(u); s/\ell, \sqrt{z})\|_{\infty, B \times E_j}.$$

Now Lemma 5.5 implies that

$$\|V(\phi_{j,i}(u); s/\ell, \sqrt{z}) - z^{n_{j,i}/2} e^{-\kappa_i s}\|_{\infty, B \times E_j} < C_{j,i}$$

for all $\ell > \ell_0$ and thus

$$\|K(s/\ell, \sqrt{z}, \ell)\|_{\infty, B} \leq \max_{j \rightsquigarrow i} \left(\|z^{n_{j,i}/2} e^{-\kappa_i s}\|_{\infty, B} + C_{j,i} \right) =: K_B.$$

As a second step we use that $\lfloor n/6 \rfloor \geq (n-5)/6$ and obtain

$$\|\tilde{d}_{\mathbf{n}}^{(k)}(s/\ell, z, \ell)\|_{\infty, B} \leq k^{k/2} K_B^k r(\ell)^{-5k/6} \sum_{m_1 < \dots < m_k} \left(r(\ell)^{1/6} \right)^{m_1 + \dots + m_k}.$$

Setting $\tilde{r}(\ell) = r(\ell)^{1/6}$ and using the Euler formula this gives

$$\|\tilde{d}_{\mathbf{n}}^{(k)}(s/\ell, z, \ell)\|_{\infty, B} \leq k^{k/2} K_B^k \tilde{r}(\ell)^{-5k} \frac{\tilde{r}(\ell)^{k(k-1)/2}}{(1 - \tilde{r}(\ell)) \dots (1 - \tilde{r}(\ell)^k)}$$

which allows us to obtain an estimate for $k \geq 12$

$$\left\| \sum_{k=12}^{\infty} \tilde{d}_{\mathbf{n}}^{(k)}(s/\ell, z, \ell) \right\|_{\infty, B} \leq \tilde{r}(\ell) \sum_{k=12}^{\infty} k^{k/2} K_B^k \frac{\tilde{r}(\ell)^{k(\frac{k-1}{2} - 5 - \frac{1}{k})}}{(1 - \tilde{r}(\ell)) \dots (1 - \tilde{r}(\ell)^k)}.$$

If $k \geq 12$ then we have $(\frac{k-1}{2} - 5 - \frac{1}{k}) > 0$ and every term in the sum is uniformly bounded for all $\ell \geq \ell_0$. Furthermore since the terms in the series decay super-exponentially in k thanks to the term $\tilde{r}(\ell)^{k^2}$ the series converges with a uniform bound and the factor $\tilde{r}(\ell)$ in front assures the convergence to zero.

It remains thus to prove that the coefficients for $7 \leq k \leq 11$ vanish. This can be seen as follows. Note that we can estimate

$$\sum_{m_1 < \dots < m_k} r(\ell)^{\lfloor m_1/6 \rfloor + \dots + \lfloor m_k/6 \rfloor} \leq \left(\sum_{m>0} r(\ell)^{\lfloor m/6 \rfloor} \right)^k \leq C_k$$

for all $\ell > \ell_0$ with $C_k := \max_{\ell > \ell_0} (6/(1-r(\ell))^k)$ independent of ℓ . We can thus write for $k > 6$

$$\begin{aligned} \sum_{m_1 < \dots < m_k} r(\ell)^{\lfloor m_1/6 \rfloor + \dots + \lfloor m_k/6 \rfloor} &= \sum_{m_1 < \dots < m_{k-1}} r(\ell)^{\lfloor m_1/6 \rfloor + \dots + \lfloor m_{k-1}/6 \rfloor} \sum_{m_k > m_{k-1}} r(\ell)^{\lfloor m_k/6 \rfloor} \\ &\leq C_{k-1} \sum_{m_k \geq 6} r(\ell)^{\lfloor m_k/6 \rfloor} \\ &= C_{k-1} \frac{6\tilde{r}(\ell)}{1-\tilde{r}(\ell)}. \end{aligned}$$

Here we used crucially that from $k \geq 7$ we have $m_k \geq 6$ and thus can obtain the bound on the sum over m_k . We have finally shown (5.11) and finished the proof of Lemma 5.6. \square

In order to prove Theorem 1.3 it finally remains to prove that

$$\lim_{\ell \rightarrow \infty} \left\| 1 + \sum_{k=1}^6 \tilde{d}_{\mathbf{n}}^{(k)}(s/\ell, \sqrt{z}; \ell) - P_{n_1, n_2, n_3}(ze^{-s}) \right\|_{\infty, B} = 0.$$

Recall that from (3.11) we have

$$\tilde{d}_{\mathbf{n}}^{(k)}(s/\ell, \sqrt{z}; \ell) = \sum_{m=1}^k \left(\sum_{(n_1, \dots, n_m) \in P(k, m)} \frac{(-1)^m}{m!} \prod_{l=1}^m \frac{1}{n_l} \sum_{w \in \mathcal{W}_{n_l}^{cl}} \frac{V_w(u_w; s/\ell, \sqrt{z})}{1 - \phi'_w(u_w)} \right), \quad (5.12)$$

so we can explicitly calculate the cycle expansion coefficients in terms of dynamical quantities of the holomorphic IFS. As the symbolic dynamics of the flow-adapted IFS directly implies that the set of closed words is empty for uneven word length this drastically reduces the complexity of the calculations: First of all only coefficients $\tilde{d}_{\mathbf{n}}^{(k)}$ with $k = 2, 4, 6$ can be nonzero, because otherwise at least one summand n_l is uneven and consequently one factor in the product $\prod_{l=1}^m$ is zero. Additionally this condition reduces the number of possible tuples (n_1, \dots, n_m) which lead to nonzero contributions drastically: For $k = 2$ it remains only the one tuple (2), for $k = 4$ there are two possibilities (4) and (2, 2) and for $k = 6$ there are four possible tuples, namely (6), (4, 2), (2, 4) and (2, 2, 2). Even if each coefficient is only given by an explicit finite sum and even if the complexity of this sums is tremendously reduced by the above discussion it remains still very complex as the number of closed words increases exponentially. As $\#\mathcal{W}_2^{cl} = 12$, $\#\mathcal{W}_4^{cl} = 36$ and $\#\mathcal{W}_6^{cl} = 132$, the coefficient $\tilde{d}_{\mathbf{n}}^{(6)}$ would a priori be given by $132 + 12 \cdot 36 + 36 \cdot 12 + 12^3 = 2724$ summands. The following Lemma however allows to reduce the complexity in the limit $\ell \rightarrow \infty$ strongly.

Lemma 5.7. *Let us define for any $n \in \mathbb{N}$*

$$\mathbf{n} : \begin{cases} \mathcal{W}_n^{cl} & \rightarrow \mathbb{N} \\ (w_0, \dots, w_n) & \mapsto \frac{1}{2} \sum_{r=0}^{n-1} n_{w_r, w_{r+1}} \end{cases}. \quad (5.13)$$

Then for any finite closed word $w \in \mathcal{W}_n^{cl}$ for the symbolic dynamics of the flow-adapted IFS and any $B \subset \mathbb{C}^2$ we have

$$\lim_{\ell \rightarrow \infty} \left\| \frac{V_w(u_w; s/\ell, \sqrt{z})}{1 - \phi'_w(u_w)} - (ze^{-s})^{\mathbf{n}(w)} \right\|_{\infty, B} = 0. \quad (5.14)$$

Remark 5.8. The notation of the application $\mathbf{n} : \mathcal{W}_k^{cl} \rightarrow \mathbb{N}$ does not only coincide by chance with the notation of the order function on the closed geodesic which was defined in (1.2). In fact if w is a prime word, then Proposition 4.4 associates this word to a primitive geodesic in $\mathcal{P}_{X_{n_1, n_2, n_3}}(\ell)$. The definition (5.13) of the order function restricted to the subset of prime words $\mathcal{W}_k^{\text{prime}}$ is then equal to the order function (1.2) on primitive geodesics with respect to this identification.

Proof. Let us first note that from the fact that $r_i \rightarrow 0$ we conclude for any $w \in \mathcal{W}_n^{cl}$ that $\lim_{\ell \rightarrow \infty} \phi'_w(u_w) = 0$. It thus only remains to handle the term $V_w(u_w; s/\ell, \sqrt{z})$ and as a first step we note that as $u_w \in D_{w_0} \subset E_{w_0}$, Lemma 5.5 implies that

$$\lim_{\ell \rightarrow \infty} \left\| V(\phi_{w_0, w_1}(u_w), s/\ell, \sqrt{z}) - z^{n_{w_0, w_1}/2} e^{-\kappa_{w_1} s} \right\|_{\infty, B} = 0. \quad (5.15)$$

From the definition (3.5) of the iterated product we obtain

$$\begin{aligned} V_w(u_w; s/\ell, \sqrt{z}) &:= \prod_{k=1}^n V(\phi_{w_0, k}(u_w); s/\ell, \sqrt{z}) \\ &= \prod_{k=1}^n V(\phi_{w_{k-1}, w_k}(u_{\sigma_L^{(k-1)} w}); s/\ell, \sqrt{z}). \end{aligned}$$

Here we used that the dynamics on the fixed points is conjugated to the shift operation (see (3.2)). Plugging in (5.15) we obtain

$$\lim_{\ell \rightarrow \infty} \left\| V_w(u_w; s/\ell, \sqrt{z}) - z^{\frac{1}{2}(\sum_{k=1}^n n_{w_{k-1}, w_k})} e^{-s(\sum_{k=1}^n \kappa_{w_k})} \right\|_{\infty, B} = 0.$$

Thus it only remains to show that $\sum_{k=1}^n \kappa_{w_k} = \mathbf{n}(w)$ in order to finish the proof. This can finally be seen as follows. First one checks that for any $i \rightsquigarrow j$ we have $\kappa_i + \kappa_j = n_{i,j}$. Secondly as $w_0 = w_n$ we can write

$$\sum_{k=1}^n \kappa_{w_k} = \frac{1}{2} \sum_{k=1}^n \kappa_{w_{k-1}} + \kappa_{w_k} = \frac{1}{2} \sum_{k=1}^n n_{w_{k-1}, w_k} = \mathbf{n}(w).$$

□

Remark 5.9. The identity $\sum_{k=1}^n \kappa_{w_k} = \mathbf{n}(w)$ shows that we could also have taken another definition of the potential functions for the generalized zeta functions namely $V(u) = z^{2\kappa_j} [-(\phi^{-1})'(u)]^{-s}$ for $u \in \phi_{i,j}(D_i)$. Note that however the κ_i are only positive if the n_i fulfill the triangle condition as defined in Lemma 5.1. In those cases where it is not satisfied the analyticity of the generalized zeta function would have been much harder to prove, so we chose the definition by the $n_{i,j}$.

We are now ready to proof Theorem 1.3.

Proof of Theorem 1.3. Lemma 5.7 implies that the w dependent terms in (5.12) depend only on $\mathbf{n}(w)$ in the limit $\ell \rightarrow \infty$. We thus introduce for any $k, n \in N$ the sets

$$\mathcal{W}_k^{cl}(n) := \{w \in \mathcal{W}_k^{cl}, \mathbf{n}(w) = n\}.$$

and observe that the relevant set of words split into

$$\mathcal{W}_2^{cl} = \mathcal{W}_2^{cl}(n_1) \cup \mathcal{W}_2^{cl}(n_2) \cup \mathcal{W}_2^{cl}(n_3) \quad (5.16)$$

$$\begin{aligned} \mathcal{W}_4^{cl} &= \mathcal{W}_4^{cl}(2n_1) \cup \mathcal{W}_4^{cl}(2n_2) \cup \mathcal{W}_4^{cl}(2n_3) \cup \\ &\quad \mathcal{W}_4^{cl}(n_1 + n_2) \cup \mathcal{W}_4^{cl}(n_2 + n_3) \cup \mathcal{W}_4^{cl}(n_1 + n_3) \end{aligned} \quad (5.17)$$

$$\begin{aligned} \mathcal{W}_6^{cl} &= \mathcal{W}_6^{cl}(3n_1) \cup \mathcal{W}_6^{cl}(3n_2) \cup \mathcal{W}_6^{cl}(3n_3) \cup \\ &\quad \mathcal{W}_6^{cl}(2n_1 + n_2) \cup \mathcal{W}_6^{cl}(n_1 + 2n_2) \cup \mathcal{W}_6^{cl}(2n_2 + n_3) \cup \mathcal{W}_6^{cl}(n_2 + 2n_3) \cup \\ &\quad \mathcal{W}_6^{cl}(2n_1 + n_3) \cup \mathcal{W}_6^{cl}(n_1 + 2n_3) \cup \mathcal{W}_6^{cl}(n_1 + n_2 + n_3) \end{aligned} \quad (5.18)$$

where the number of elements per set is given by

$$\begin{aligned} \#\mathcal{W}_2(n_j) = \#\mathcal{W}_4(2n_j) = \#\mathcal{W}_6(3n_j) &= 4 \quad \forall 1 \leq j \leq 3 \\ \#\mathcal{W}_4(n_i + n_j) &= 8 \quad \forall 1 \leq i, j \leq 3 \text{ with } i \neq j \\ \#\mathcal{W}_6(2n_i + n_j) &= 12 \quad \forall 1 \leq i, j \leq 3 \text{ with } i \neq j \\ \#\mathcal{W}_6(n_1 + n_2 + n_3) &= 48 \end{aligned} \quad (5.19)$$

One can convince oneself from the validity of these formulas by geometric arguments. For example the only closed geodesics, that intersect only two of the blue lines in Figure 5.3 are those who make one circle around one of the three funnels. As the closed words correspond to closed geodesics, the closed words of order two split according to (5.16). Around each funnel there are two different geodesics (one in each sense of orientation) and each geodesic is encoded by two different words which leads to $\mathcal{W}_2^{cl}(n_i) = 4$. All other results can be understood by similar arguments, the easiest way to calculate (5.16)-(5.19) is however to solve the finite combinatorial problem exactly with a computer.

With this data it is a straight forward task to calculate that

$$\left\| \tilde{d}_{\mathbf{n}}^{(2)}(s/\ell, \sqrt{z}; \ell) + 2 \left[(ze^{-s})^{n_1} + (ze^{-s})^{n_2} + (ze^{-s})^{n_3} \right] \right\|_{\infty, B} = 0 \quad (5.20)$$

$$\begin{aligned} &\left\| \tilde{d}_{\mathbf{n}}^{(4)}(s/\ell, \sqrt{z}; \ell) - \left[(ze^{-s})^{2n_1} + (ze^{-s})^{2n_2} + (ze^{-s})^{2n_3} + \right. \right. \\ &\quad \left. \left. 2 \left((ze^{-s})^{n_1+n_2} + (ze^{-s})^{n_1+n_3} + (ze^{-s})^{n_2+n_3} \right) \right] \right\|_{\infty, B} = 0 \end{aligned} \quad (5.21)$$

$$\left\| \tilde{d}_{\mathbf{n}}^{(6)}(s/\ell, \sqrt{z}; \ell) + 4(ze^{-s})^{n_1+n_2+n_3} \right\|_{\infty, B} = 0 \quad (5.22)$$

Equation (5.20) is seen immediately because as discussed above the only possible tuple (n_1, \dots, n_m) is the one-tuple (2). The next equation (5.21) can be seen as follows: First

we split (5.12) according to the two possible tuples (4) and (2, 2)

$$\tilde{d}_{\mathbf{n}}^{(4)}(s/\ell, \sqrt{z}; \ell) = \underbrace{-\frac{1}{4} \left(\sum_{w \in \mathcal{W}_4^{cl}} \frac{V_w(u_w; s/\ell, \sqrt{z})}{1 - \phi'_w(u_w)} \right)}_{(A)} + \underbrace{\frac{1}{2!} \left(\frac{1}{2} \sum_{w \in \mathcal{W}_2^{cl}} \frac{V_w(u_w; s/\ell, \sqrt{z})}{1 - \phi'_w(u_w)} \right)^2}_{(B)}.$$

Next we treat the parts (A) and (B) separately. For (A) we use (5.17) and obtain

$$\begin{aligned} (A) &= -\frac{1}{4} \left(\sum_{w \in \mathcal{W}_4^{cl}(2n_1)} \left[\frac{V_w(u_w; s/\ell, \sqrt{z})}{1 - \phi'_w(u_w)} - (ze^{-s})^{2n_1} \right] + \right. \\ &\quad \sum_{w \in \mathcal{W}_4^{cl}(2n_2)} \left[\frac{V_w(u_w; s/\ell, \sqrt{z})}{1 - \phi'_w(u_w)} - (ze^{-s})^{2n_2} \right] + \\ &\quad \sum_{w \in \mathcal{W}_4^{cl}(2n_3)} \left[\frac{V_w(u_w; s/\ell, \sqrt{z})}{1 - \phi'_w(u_w)} - (ze^{-s})^{2n_3} \right] + \\ &\quad \sum_{w \in \mathcal{W}_4^{cl}(n_1+n_2)} \left[\frac{V_w(u_w; s/\ell, \sqrt{z})}{1 - \phi'_w(u_w)} - (ze^{-s})^{n_1+n_2} \right] + \\ &\quad \sum_{w \in \mathcal{W}_4^{cl}(n_2+n_3)} \left[\frac{V_w(u_w; s/\ell, \sqrt{z})}{1 - \phi'_w(u_w)} - (ze^{-s})^{n_2+n_3} \right] + \\ &\quad \left. \sum_{w \in \mathcal{W}_4^{cl}(n_1+n_3)} \left[\frac{V_w(u_w; s/\ell, \sqrt{z})}{1 - \phi'_w(u_w)} - (ze^{-s})^{n_1+n_3} \right] - \right. \\ &\quad \left. \left[4(ze^{-s})^{2n_1} + 4(ze^{-s})^{2n_2} + 4(ze^{-s})^{2n_3} + 8(ze^{-s})^{n_1+n_2} + 8(ze^{-s})^{n_2+n_3} + 8(ze^{-s})^{n_1+n_3} \right] \right). \end{aligned}$$

In order to treat (B) we use (5.16) and calculate

$$\begin{aligned} (B) &= +\frac{1}{2} \left(\frac{1}{2} \sum_{w \in \mathcal{W}_2^{cl}(n_1)} \left[\frac{V_w(u_w; s/\ell, \sqrt{z})}{1 - \phi'_w(u_w)} - (ze^{-s})^{n_1} \right] + \right. \\ &\quad \frac{1}{2} \sum_{w \in \mathcal{W}_2^{cl}(n_2)} \left[\frac{V_w(u_w; s/\ell, \sqrt{z})}{1 - \phi'_w(u_w)} - (ze^{-s})^{n_2} \right] + \\ &\quad \frac{1}{2} \sum_{w \in \mathcal{W}_2^{cl}(n_3)} \left[\frac{V_w(u_w; s/\ell, \sqrt{z})}{1 - \phi'_w(u_w)} - (ze^{-s})^{n_3} \right] + \\ &\quad \left. \left[2(ze^{-s})^{n_1} + 2(ze^{-s})^{n_2} + 2(ze^{-s})^{n_3} \right] \right)^2. \end{aligned}$$

Note that in both equations of (A) and (B), respectively, all terms except the last line converge uniformly to 0 on the set $B \subset \mathbb{C}^2$. So the limit $\ell \rightarrow \infty$ the coefficient

$\tilde{d}_{\mathbf{n}}^{(4)}(s/\ell, \sqrt{z}; \ell)$ converges uniformly to

$$\begin{aligned} & -\frac{1}{4} [4(ze^{-s})^{2n_1} + 4(ze^{-s})^{2n_2} + 4(ze^{-s})^{2n_3} + 8(ze^{-s})^{n_1+n_2} + 8(ze^{-s})^{n_2+n_3} + 8(ze^{-s})^{n_1+n_3}] \\ & + \frac{1}{2} [2(ze^{-s})^{n_1} + 2(ze^{-s})^{n_2} + 2(ze^{-s})^{n_3}]^2 \\ & = (ze^{-s})^{2n_1} + (ze^{-s})^{2n_2} + (ze^{-s})^{2n_3} + 2(ze^{-s})^{n_1+n_2} + 2(ze^{-s})^{n_2+n_3} + 2(ze^{-s})^{n_1+n_3} \end{aligned}$$

which proves (5.21). By a completely analogous but more tedious calculation we can show (5.22).

Finally we can put (5.20), (5.21) and (5.22) together and obtain (1.4) which finishes the proof of Theorem 1.3. \square

Remark 5.10. Note that the limit form of $\frac{V_w(u_w; s/\ell, \sqrt{z})}{1-\phi_w'(u_w)}$ in (5.14) of Lemma 5.7 not only allows to group many terms together but also allows to take advantage of a systematic canceling. For example in the calculation of $\tilde{d}_{\mathbf{n}}^{(4)}(s/\ell, \sqrt{z}; \ell)$ the terms $(ze^{-s})^{(n_1+n_2)}$ appears as limits of two different geodesics. First they appear in the term (A) as limits of the eight-shaped geodesics which turn around the funnels of width n_1 and n_2 (see green geodesic in Figure 5.3). Secondly they appear in (B) as the product of the geodesic which turns once around the funnel of width n_1 with another geodesic which turns once around the funnel of width n_2 (see the two red geodesics in Figure 5.3). As both terms appear with different signs they cancel each other to a big extent. Note that this cancellation is not exactly true for finite ℓ . In the setting of the physical quantum 3-disk system it has however been argued that this cancellation is approximately true. The mechanism that the contribution of longer orbits is approximately canceled by a combination of shorter orbits which Cvitanovic and Eckhardt call *shadowing orbits* has been identified in physics literature as the key mechanism for the fast convergence of the cycle expansion. Lemma 5.7 can thus also be seen as a proof that in the limit $\ell \rightarrow \infty$ this approximation becomes exact on Schottky surfaces.

Theorem 1.1 on the location of the rescaled resonances now follows directly from Theorem 1.3.

Proof of Theorem 1.1. Recall that

$$\mathcal{N}_{n_1, n_2, n_3} = \{s \in \mathbb{C}, P_{n_1, n_2, n_3}(e^{-s}) = 0\}$$

and

$$\widetilde{\text{Res}}_{n_1, n_2, n_3}(\ell) := \{s \in \mathbb{C}, s/\ell \in \text{Res}(X_{n_1, n_2, n_3}(\ell))\}.$$

If $U \subset \mathbb{C}$ is a domain whose boundary ∂U is disjoint with $\mathcal{N}_{n_1, n_2, n_3}$ then the argument principle implies that

$$\#(U \cap \mathcal{N}_{n_1, n_2, n_3}) = \frac{1}{2\pi i} \int_{\partial U} \frac{f'(s)}{f(s)} ds$$

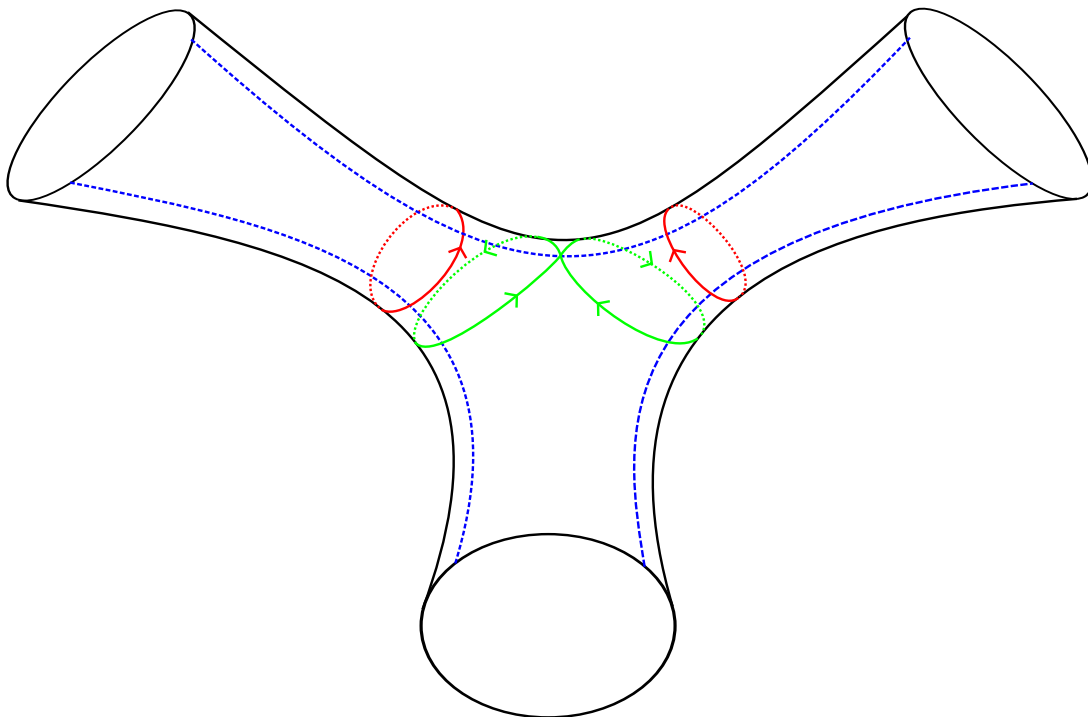


Figure 5.3: Schematic sketch of a 3-funneled Schottky surface. The blue, dashed lines indicate the cut lines of the Poincaré section which would correspond to the flow-adapted IFS. In red we see two geodesics which make one turn around one funnel each. They correspond to the closed words of length 2 $w^{(a)} = (1, 5, 1)$ and $w^{(b)} = (3, 5, 3)$. In green we see a geodesic which winds around both funnels in an eight-like shape. It corresponds to the closed word $w^{(c)} = (1, 5, 3, 5, 1)$ of length 4. Note that $\mathbf{n}(w^{(a)}) + \mathbf{n}(w^{(b)}) = \mathbf{n}(w^{(c)})$.

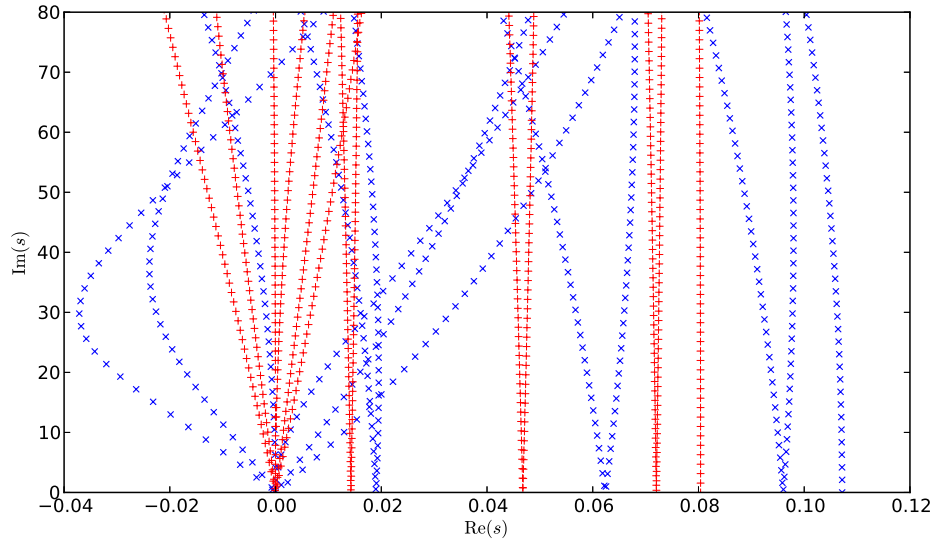


Figure 6.1: Resonance spectrum for the surfaces $X_{4,4,5}(\ell)$ for $\ell = 3$ (blue crosses) and $\ell = 4$ (red plus signs).

with $f(s) = P_{n_1, n_2, n_3}(e^{-s})$. On the other hand

$$\#(U \cap \widetilde{\text{Res}}_{n_1, n_2, n_3}(\ell)) = \int_{\partial U} \frac{\frac{d}{ds} Z_{X_{n_1, n_2, n_3}(\ell)}(s/\ell)}{Z_{X_{n_1, n_2, n_3}(\ell)}(s/\ell)} ds$$

and Theorem 1.3 implies that

$$Z_{X_{n_1, n_2, n_3}(\ell)}(s/\ell) = d_{\mathbf{n}}(s/\ell, 1) \rightarrow f(s)$$

uniformly on ∂U . This in turn immediately implies Theorem 1.1. \square

6 Numerical Illustration

In this section we will test the convergence of the rescaled spectrum towards the zeros of the polynomials P_{n_1, n_2, n_3} . The resonances are calculated by finding the zeros of the Selberg zeta function with the same algorithm as used by Borthwick [4] (see also [15, 13]) which has been implemented in python, using Sage [28] and the scipy/numpy [16] package.

In Figure 6.1 we see the resonance spectrum of the surface $X_{4,4,5}(\ell)$ for two different ℓ -values ($\ell = 3$ as blue crosses, and $\ell = 4$ in red plus signs). Both plots show significant resonance chains. However, without rescaling, these chains are clearly different. The

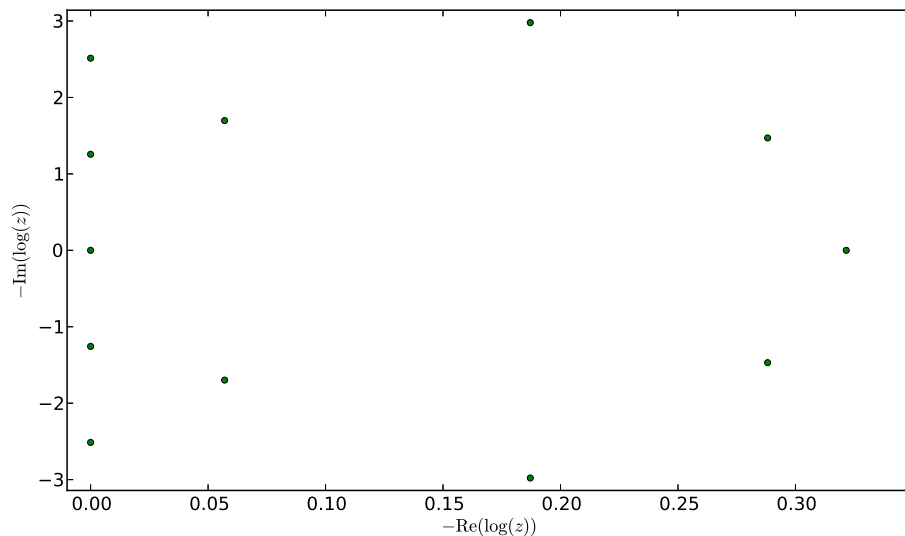


Figure 6.2: Solutions of the equation $P_{4,4,5}(z) = 0$ plotted on a negative logarithmic scale. The zero at $\log(z) = 0$ is of order two.

chains for $\ell = 4$ are denser and are positioned at significantly smaller real part and are much less curved than the chains for $\ell = 3$. Their rough structure is however very similar. From higher to lower real parts, both surfaces first have a single chain, then three pairs of chains that diverge from each other and finally six resonance chains that emerge from $s = 0$. This common structure can be completely understood by the zeros of the polynomial

$$P_{4,4,5}(z) = -4z^{13} + z^{10} + 4z^9 + 4z^8 - 2z^5 - 4z^4 + 1.$$

Figure 6.2 shows the solutions of $P_{4,4,5}(z) = 0$. As Theorem 1.1 provides a connection between the resonances and the zeros of $P(e^{-s})$ we have plotted $-\log(z)$ in order to compare the structure of the zeros directly with the resonances. And indeed the structure of the zeros of $P_{4,4,5}$ is exactly the same as the resonance chain structure. From higher to lower real parts (in the negative logarithmic plot of Figure 6.2) there is one leading zero, then three pairs of zeros which have the same real part and finally 5 zeros with real part equal to zero of which the zero with $\log(z) = 0$ is of order two. But not only the rough resonance structure is described by the zeros of $P_{4,4,5}$, also a large part of the rescaled spectrum is quantitatively well described by the zeros of $P_{4,4,5}(e^{-s})$. Figure 6.3 shows the rescaled spectrum for $\ell = 3$ and $\ell = 4$. Additionally the zeros of $P_{4,4,5}(e^{-s})$ are plotted in green circles. One sees that in the plot range already for $\ell = 4$ the first 7 rescaled chains do very well coincide with their limit

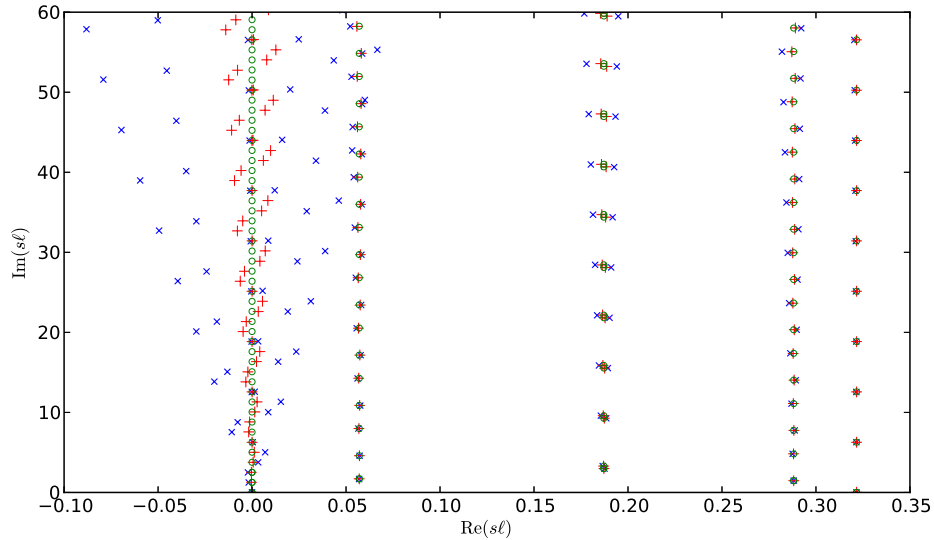


Figure 6.3: Rescaled resonances for the surface $X_{4,4,5}(\ell)$ for $\ell = 3$ (blue crosses) and $\ell = 4$ (red plus signs). Additionally the green circles indicate the zeros of the polynomial $P_{4,4,5}(e^{-s})$ in the plot range. One observes that the resonances of the different surfaces really lie on approximately the same points after rescaling and that the zeros of the polynomial $P_{4,4,5}(e^{-s})$ predict the position of most of the resonances for $\ell = 4$ already very well.

values given by $P_{4,4,5}$. Only the chains emerging from zero are still very unstable and show a visible difference. Overall however more than 70 resonances in the plot range are quantitatively well described by $P_{4,4,5}$. For $\ell = 3$ the discrepancy is, as expected, higher however all resonances on the first chain are also very well approximated.

As a second example we show the same plots for the surfaces $X_{4,5,6}(\ell)$, this time for $\ell = 4$ and $\ell = 5$ (see Figure 6.4, 6.5 and 6.6). The corresponding polynomial is now given by

$$P_{4,5,6}(z) = -4z^{15} + z^{12} + 2z^{11} + 3z^{10} + 2z^9 + z^8 - 2z^6 - 2z^5 - 2z^4 + 1.$$

As this surface is even less symmetric, the zeros of the polynomial has an even more complex structure (Figure 6.5). Now there is one leading zero, then 6 pairs of zeros and finally a zero of order two at $\log(z) = 0$. This corresponds exactly to the more complex chain structure with one leading chain and 7 further pairs of chains (Figure 6.4). Finally, after rescaling, the position of a large part part of the plotted resonances agrees with the zeros of $P_{4,5,6}(e^{-s})$ (see Figure 6.6).

Increasing the parameter ℓ even further yields a better and better coincidence be-

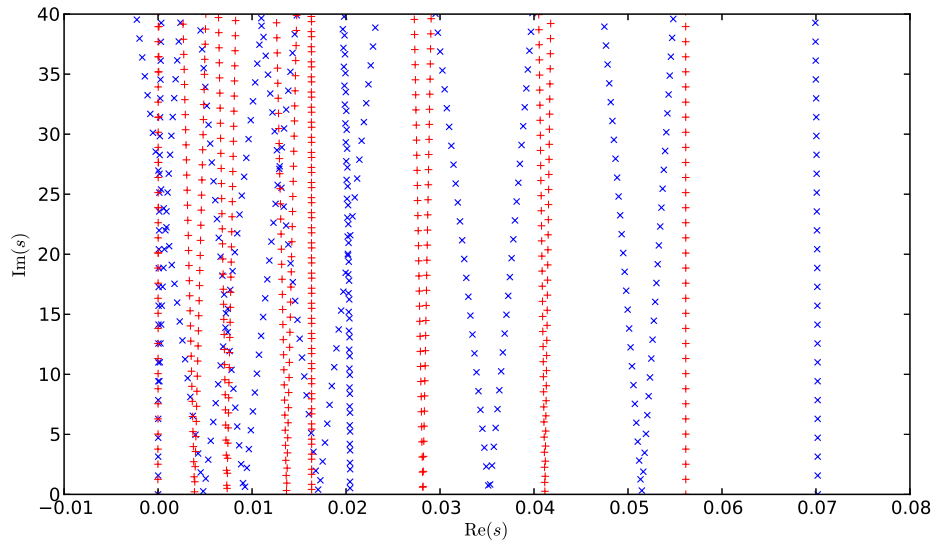


Figure 6.4: Resonance spectrum for the surfaces $X_{4,5,6}(\ell)$ for $\ell = 4$ (blue crosses) and $\ell = 5$ (red plus signs).

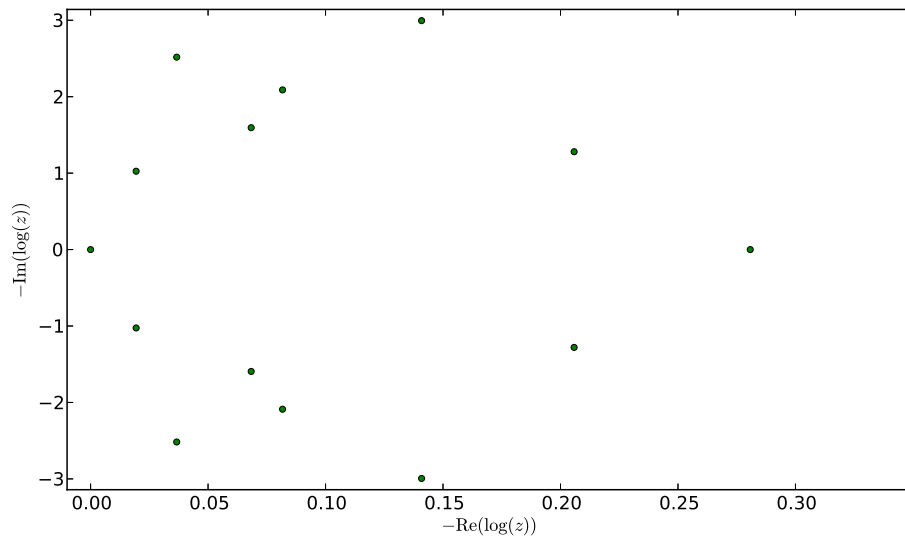


Figure 6.5: Solutions of the equation $P_{4,5,6}(z) = 0$ plotted on a negative logarithmic scale. The zero at $\log(z) = 0$ is of order two.

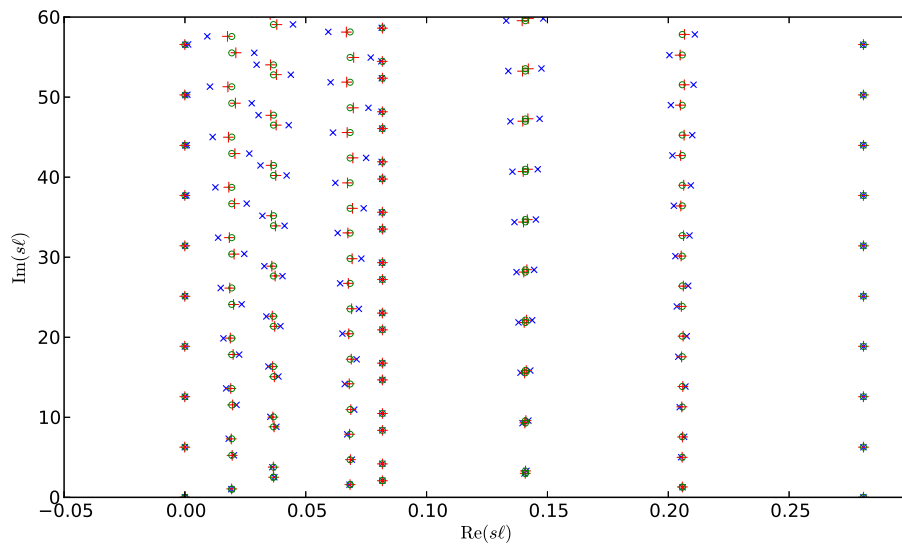


Figure 6.6: Rescaled resonances for the surface $X_{4,5,6}(\ell)$ for $\ell = 4$ (blue crosses) and $\ell = 5$ (red plus signs). Additionally the green circles indicate the zeros of the polynomial $P_{4,5,6}(e^{-s})$ in the plot range. One observes that the resonances of the different surfaces lie on approximately the same points after rescaling and that the zeros of the polynomial $P_{4,5,6}(e^{-s})$ predict the position of most of the resonances for $\ell = 5$ already very well.

tween the numerically calculated resonances and those predicted by the polynomial. For the surface $X_{12,12,12}$ we checked for example that the position of more than 150 individual resonances can be determined at a precision of 10^{-3} by calculating the zeros of the polynomial

$$P_{1,1,1}(z) = -4z^3 + 9z^2 - 6z + 1 = -(z-1)^2(4z-1)$$

which can in this case even be factorized by hand.

References

- [1] S. Barkhofen, F. Faure, and T. Weich. Resonance chains in open systems, generalized zeta functions and clustering of the length spectrum. *In preparation*.
- [2] S. Barkhofen, T. Weich, A. Potzuweit, H-J. Stöckmann, U. Kuhl, and M. Zworski. Experimental observation of the spectral gap in microwave n-disk systems. *Physical review letters*, 110(16):164102, 2013.
- [3] D. Borthwick. *Spectral theory of infinite-area hyperbolic surfaces*. Basel: Birkhäuser, 2007.
- [4] D. Borthwick. Distribution of resonances for hyperbolic surfaces. *Experimental Mathematics*, 23:25–45, 2014.
- [5] D. Borthwick, C. Judge, and P.A. Perry. Selberg’s zeta function and the spectral geometry of geometrically finite hyperbolic surfaces. *Comment. Math. Helv.*, 80:483–515, 2005.
- [6] D. Borthwick and T. Weich. Symmetry reduction of holomorphic iterated function schemes and factorization of Selberg zeta functions. *In preparation*.
- [7] J. Bourgain, A. Gamburd, and P. Sarnak. Generalization of Selberg’s $\frac{3}{16}$ theorem and affine sieve. *Acta mathematica*, 207(2):255–290, 2011.
- [8] U. Bunke and M. Olbrich. Group cohomology and the singularities of the Selberg zeta function associated to a kleinian group. *Annals of mathematics*, 149:627–689, 1999.
- [9] P. Cvitanović and B. Eckhardt. Periodic-orbit quantization of chaotic systems. *Physical review letters*, 63(8):823–826, 1989.
- [10] P. Gaspard and S.A. Rice. Semiclassical quantization of the scattering from a classically chaotic repeller. *The Journal of chemical physics*, 90:2242, 1989.
- [11] A. Grothendieck. La théorie de fredholm. *Bulletin de la Société Mathématique de France*, 84:319–384, 1956.
- [12] L. Guillopé. Fonctions zêta de selberg et surfaces de géométrie finie. *Adv. Stud. Pure Math*, 21:33–70, 1992.

- [13] L. Guillopé, K.K. Lin, and M. Zworski. The Selberg zeta function for convex co-compact Schottky groups. *Communications in mathematical physics*, 245(1):149–176, 2004.
- [14] L. Guillopé and M. Zworski. Upper bounds on the number of resonances for non-compact Riemann surfaces. *J. Funct. Anal.*, 129(2):364–389, 1995.
- [15] O. Jenkinson and M. Pollicott. Calculating Hausdorff dimension of Julia sets and Kleinian limit sets. *American Journal of Mathematics*, 124(3):495–545, 2002.
- [16] E. Jones, T. Oliphant, P. Peterson, et al. SciPy: Open source scientific tools for Python, 2001–.
- [17] WT Lu, S. Sridhar, and M. Zworski. Fractal Weyl laws for chaotic open systems. *Physical review letters*, 91(15):154101, 2003.
- [18] R.R. Mazzeo and R.B. Melrose. Meromorphic extension of the resolvent on complete spaces with asymptotically constant negative curvature. *Journal of Functional analysis*, 75(2):260–310, 1987.
- [19] C.T. McMullen. Hausdorff dimension and conformal dynamics, III: Computation of dimension. *American journal of mathematics*, pages 691–721, 1998.
- [20] F. Naud. Expanding maps on Cantor sets and analytic continuation of zeta functions. *Ann. Sci. Éc. Norm. Supér. (4)*, 38(1):116–153, 2005.
- [21] S. Nonnenmacher. Spectral problems in open quantum chaos. *Nonlinearity*, 24(12):R123, 2011.
- [22] S.J. Patterson. The limit set of a Fuchsian group. *Acta mathematica*, 136(1):241–273, 1976.
- [23] S.J. Patterson. On a lattice-point problem in hyperbolic space and related questions in spectral theory. *Arkiv för Matematik*, 26(1):167–172, 1988.
- [24] S.J. Patterson and P.A. Perry. The divisor of Selberg’s zeta function for Kleinian groups. Appendix A by Charles Epstein. *Duke Math. J.*, 106(2):321–390, 2001.
- [25] A. Potzweit, T. Weich, S. Barkhofen, U. Kuhl, H.-J. Stöckmann, and M. Zworski. Weyl asymptotics: From closed to open systems. *Physical Review E*, 86(6):066205, 2012.
- [26] D. Ruelle. Zeta-functions for expanding maps and Anosov flows. *Inventiones mathematicae*, 34(3):231–242, 1976.
- [27] H. Schomerus and J. Tworzydło. Quantum-to-classical crossover of quasibound states in open quantum systems. *Physical review letters*, 93(15):154102, 2004.
- [28] W. A. Stein et al. *Sage Mathematics Software (Version 6.1.1)*. The Sage Development Team, 2014. <http://www.sagemath.org>.

- [29] W.P. Thurston. *The Geometry and Topology of Three-Manifolds*. <http://www.msri.org/publications/books/gt3m/>, electronic version 1.1 edition, 2002.
- [30] T. Weich, S. Barkhofen, U. Kuhl, C. Poli, and H. Schomerus. Formation and interaction of resonance chains in the open 3-disk system. *New Journal of Physics*, 16:033029, 2014.